August 8, 1974

To the Graduate Council:

I am submitting herewith a thesis written by Vijaysinh Vasanji Badamwala entitled "The Measurement of Interfacial Area in Concurrent Gas-Liquid Flow Through Packed Beds." I recommend that it be accepted in partial fulfillment of the requirements for the degree of Master of Science, with a major in Chemical Engineering.

J. J. Perona

J. J. Perona, Major Professor

We have read this thesis
and recommend its acceptance:

George C. Fazio

H. W. Haw

Accepted for the Council:

Hilton A. Smith

Vice Chancellor for
Graduate Studies and Research

THE MEASUREMENT OF INTERFACIAL AREA IN CONCURRENT GAS-LIQUID FLOW THROUGH PACKED BEDS

A Thesis

Presented to

the Graduate Council of

The University of Tennessee

In Partial Fulfillment

of the Requirements for the Degree

Master of Science

---

by

Vijaysinh Vasanji Badamwala

December 1974

ACKNOWLEDGEMENT

The author appreciates the patience, guidance, and many helpful suggestions of his research advisor, Dr. J. J. Perona. The author is also grateful to Dr. H. F. Johnson and the Department of Chemical and Metallurgical Engineering at The University of Tennessee for financial aid in the form of a graduate assistantship and to the National Science Foundation for aid in the form of a Non-Service Fellowship.

Sincere thanks are extended to all the people that make up the Chemical and Metallurgical Engineering Department at UT. Thanks are due to the Facilities Management Group--Art Freeborg, Tom Ayres and their work-study assistants. The same thanks go out to the men in Machine Shop, and special thanks to Mr. H. B. Thompson, who solved many problems I could only attempt to overcome.

I want to thank all my friends, especially John Caton, in the Department for the direct and indirect help they gave me.

1175914

ABSTRACT

Liquid-film mass transfer coefficients were measured for carbon dioxide absorption into carbonate-bicarbonate solution from an air-CO_2 mixture in a packed column operated in concurrent flow. The packed section of the column was constructed from 10.2 cm I.D. pyrex glass pipe with two different packed lengths of 25.4 cm and 91.44 cm. A majority of the data were taken by using the shorter column to minimize wall flow. The packing for all experiments was one-half inch Raschig rings. Liquid superficial velocities were varied from 0.655 cm/sec to 2.65 cm/sec and the gas velocities were varied from 13.1 cm/sec to 56.5 cm/sec. These combinations of velocities go far beyond those possible in countercurrent operation.

Both the liquid film mass transfer coefficient, k_L, and the effective interfacial area, a, were affected significantly by the liquid and gas velocities, and were somewhat higher than for countercurrent operation. Values of $k_L a$ were higher for concurrent flow by factors of two to three.

Values of $k_L a$ in the presence of a chemical reaction were higher than for physical operation. This is thought to be caused by the continued effectiveness of slow moving regions of the packed bed due to the reaction. With the taller column, values of effective interfacial area per unit volume of packing and k_L were less than for the short column, which shows that the wall effect diminishes both quantities.

TABLE OF CONTENTS

CHAPTER		PAGE
I.	INTRODUCTION	1
	Introductory Remarks	1
	Previous Work	2
	Purpose of the Investigation	8
	Scope of the Investigation	8
II.	THEORY	10
III.	EXPERIMENTAL EQUIPMENT AND PROCEDURE	19
	Details of the Equipment	19
	Experimental Procedure	23
IV.	RESULTS AND DISCUSSION	27
	Results of Liquid-Film Mass Transfer Coefficients and Effective Interfacial Area	27
	Comparison of Effective Interfacial Area and Liquid-Film Mass Transfer Coefficient with Literature	37
	Pulsing Flow	42
	Effect of Column Height	42
	Comparison with Chemical Absorption and Physical Absorption	44
V.	CONCLUSIONS	49
LIST OF REFERENCES		50
APPENDICES		54
Appendix A		55
Appendix B		67

CHAPTER PAGE

Appendix C 73

Appendix D 79

VITA 85

LIST OF TABLES

TABLE PAGE

1. Gas Superficial Velocity 13.1 cm/sec, with Height of Packing = 25.4 cm 75
2. Gas Superficial Velocity 28.25 cm/sec, with Height of Packing = 25.4 cm 76
3. Gas Superficial Velocity 56.5 cm/sec with Height of Packing = 25.4 cm 77
4. Gas Superficial Velocity 56.5 cm/sec with Height of Packing = 91.44 cm. 78
5. Calculated Intercept and Slope of the Line for Height of Packing = 25.4 81
6. Calculated Intercept and Slope of the Line for Height of Packing = 91.44 cm 82
7. Calculated Interfacial Areas and Liquid-Film Mass Transfer Coefficients for Height of Packing = 25.4 cm. 83
8. Calculated Interfacial Areas and Liquid-Film Mass Transfer Coefficients for Height of Packing = 91.44 cm. 84

LIST OF FIGURES

FIGURE		PAGE
1.	Details of the Packed Column	20
2.	Diagram of Experimental System	21
3.	Diagram of pH Versus Amount of HCl	25
4.	Absorption into Solutions Containing Hypochlorite in a Packed Column with the Gas Velocity 13.1 cm/sec.	28
5.	Absorption into Solutions Containing Hypochlorite in a Packed Column with the Gas Velocity 28.25 cm/sec	29
6.	Absorption into Solutions Containing Hypochlorite in a Packed Column with the Gas Velocity 56.5 cm/sec.	30
7.	Absorption into Solutions Containing Hypochlorite in a Packed Column 91.44 cm in Height	31
8.	Effect of Liquid Superficial Velocity on Effective Interfacial Area	32
9.	Effect of Liquid Superficial Velocity on Liquid-Film Mass Transfer Coefficient, k_L	33
10.	Effect of Gas Superficial Velocity on Effective Interfacial Area.	34
11.	Effect of Gas Superficial Velocity on Liquid-Film Mass Transfer Coefficient, k_L	35
12.	Effect of Liquid Superficial Velocity on Liquid-Phase Mass Transfer Coefficient, $k_L a$	40

FIGURE PAGE

13. Effect of Gas Superficial Velocity on Liquid-Phase Mass Transfer Coefficient, $k_L a$ 41

14. Effect of Gas Velocity and Liquid Velocity on the Flow in the Packed Column. 43

15. Effect of Height on Effective Interfacial Area 45

16. Effect of Height on Liquid-Film Mass Transfer Coefficient, k_L. 46

17. Effect of Chemical Absorption on Liquid-Phase Mass Transfer Coefficient, $k_L a$. 48

18. Liquid Rotameter Calibration Curve 69

19. CO_2 Rotameter Calibration Curve. 70

20. First Air Rotameter Calibration Curve. 71

21. Second Air Rotameter Calibration Curve 72

NOMENCLATURE

a = interfacial area per unit packed volume, cm^{-1}.

A^* = concentration of dissolved gas A at interface, in equilibrium with gas at interface, g mole/cm^3.

A° = concentration of A in bulk of liquid, g mole/cm^3.

A = concentration of A in a liquid phase in equilibrium with bulk concentration in a gas phase, g mole/cm^3.

b = concentration of reactant B, g mole/cm^3.

$\bar{b}$ = Laplace transform of $b = \int_0^\infty be^{-s\theta}\, d\theta$, g mole/$cm^3$.

B° = concentration of B in bulk of liquid, g mole/cm^3.

C = concentration of dissolved gas, A, g mole/cm^3.

D = diffusivity, cm^2/sec.

D_A = diffusivity of dissolved gas A, cm^2/sec.

D_B = diffusivity of reactant B, cm^2/sec.

E = enhancement factor, i.e., factor by which rate of absorption is increased by reaction.

G = superficial velocity of gas, cm/sec.

I = ionic strength, g ion/liter.

k_1 = first-order rate-constant of forward reaction of A, sec^{-1}.

k_c = catalytic rate-constant, l/gm mole sec.

k_G = gas phase mass transfer coefficient, g mole/cm^2 sec atm.

k_L = liquid-film mass transfer coefficient, cm/sec.

K_G = overall mass transfer coefficient based on gas side, g mole/ cm^2 sec atm.

K_L = overall mass transfer coefficient based on liquid side, cm/sec.

L = superficial velocity of liquid, cm/sec.

p = partial pressure of soluble gas A in bulk of gas, atm.

p_i = partial pressure of soluble gas A at interface, atm.

p* = partial pressure of soluble gas A in equilibrium with bulk concentration of A in liquid phase, atm.

R = rate of absorption into agitated liquid, g mole/cm^2 sec.

R_1 = rate of absorption per unit area of surface after contact time t, g mole/cm^2 sec.

s = fractional rate of surface-renewal, sec^{-1}.

x = distance beneath liquid surface, cm.

μ = viscosity of liquid g/cm sec.

ρ = density of liquid, g/cm^3.

CHAPTER I

INTRODUCTION

A. INTRODUCTORY REMARKS

Gas absorption is a fundamental process utilized in industry, and it has been applied in pollution control for many years. Considering the increasing need for more efficient pollution elimination processes, the importance of gas absorption is obvious. The vast majority of the commercial packed columns for gas-liquid contacting is operated countercurrently. The gas throughput in this type of operation is limited. Above a critical gas velocity the gravity forces on the downflowing liquid are exceeded by drag forces imposed on the liquid by the upflowing gas. This unstable condition is known as flooding and is the characteristic of all countercurrent gas-liquid contacting operation.

One means of overcoming this throughput limitation of countercurrent operation is to operate the packed column concurrently. There is no flooding limit for this type of operation and the throughput of gas and liquid up to chocked flow, depends only on the available pressure to drive the fluids through the column.

Concurrent operation appears advantageous from the fluid mechanics standpoint, whereas, from the mass-transfer standpoint, concurrent operation has a definite limitation relative to countercurrent operation. The overall concentration driving force in

countercurrent operation is greater than in concurrent operation.

In gas-liquid reaction systems the reaction of the absorbed gas after entering the liquid effectively removes it, and thus the concentration in the liquid is lowered from what it would be in purely physical absorption. The effect of this is to maintain a larger concentration difference or "driving force for transfer" between the gas and liquid phases, and the advantage of countercurrent flow is lessened. Varying degrees of this effect are possible depending on the nature of the reaction.

The prediction of rates of absorption into reacting liquids in industrial equipment under specified hydrodynamic conditions requires a separate knowledge of k_L, the liquid side mass transfer coefficient and a, the effective specific interfacial area, in the specified packing under specified operating conditions. In applying this knowledge in concurrent systems a need arises for data on liquid-side mass transfer coefficients and interfacial areas, for little work has been done in the determination of these values in concurrent flow.

B. PREVIOUS WORK

Conventional operation of packed towers has been countercurrent passage of the phases through the bed and most of the work in mass transfer has been done in countercurrent operation. The majority of the literature and texts discussing gas-liquid systems assume that the flow is countercurrent and only give brief mention to the possibility of concurrent flow and its disadvantage in mass transfer.

This is not true when absorption is accompanied by the reaction and it has been noted by Wen, et.al. (31), Dodds, et.al. (10), Reiss (22) and Gianetto, et.al. (12). Very few references related to mass transfer in concurrent operation were found in the literature. The work of Wen (31), Danckwerts (8), Dodds (10), Reiss (22), and Gianetto (12) should be noted. The work of Danckwerts and Gillham was not a study of concurrent flow mass transfer and its advantages but they measured liquid-film mass transfer coefficients and effective interfacial areas in concurrent flow.

There is much work done in mass transfer in countercurrent operation, in measuring rates of absorption (4, 5, 15, 32). Little work has been done in trying to separate liquid-film mass transfer coefficients and effective interfacial areas. The work of Shulman (21), Richards (23), Onda (16), Danckwerts (8) and Andrieu (1) should be noted.

Wen, et.al. (31) measured gas phase coefficients ($k_G a$) in dehumidification of air by calcium chloride solutions. The liquid rate varied from 4700 lb/hr. ft.^{2} to 19,200 lb/hr. ft.^{2} and gas rate varied from 224 lb/hr. ft.^{2} to 712 lb/hr. ft.^{2}. Three types of packing were used, one inch, one-half inch and one-fourth inch Raschig rings. Additional gas phase coefficients as well as liquid phase coefficients in concurrent flow were presented by Reiss (22); however, he correlated his data to energy dissipation functions which are in turn related to the two phase pressure drop correlations of Larkins (14). These new type of correlations take away much of the accuracy of predictions since they depend on the accuracy of the

two phase pressure drop correlations. The stated accuracy is ± 50 percent. Reiss measured gas phase coefficients ($k_G a$) for ammonia absorption and liquid phase coefficients ($k_L a$) for oxygen desorption with stacked and dumped one-half inch and one inch Intalox saddles. He concluded that more work is required to evaluate the effect of fluid properties on liquid holdup, radial distribution and both liquid phase and gas phase resistance controlling mass transfer capacity coefficients.

Dodds, et.al. (10) studied overall mass transfer in concurrent flow through a packed column in which the absorbed gas reacts in the liquid phase. They absorbed carbon dioxide into sodium hydroxide solution of different normalities. They used liquid flow up to 32,600 lb/hr. ft.^{2} and gas flow rate to 56.6 lb moles/hr. ft.^{2}. They found higher overall coefficients than for countercurrent flow. Their work was a statistical investigation of the variables affecting the absorption and was very limited in scope. No correlation or extensive comparison was possible from the data.

Danckwerts and Gillham (8) measured liquid-film mass transfer coefficients and effective interfacial areas. They used a buffer solution of carbonate-bicarbonate and hypochlorite as a catalyst. In their experiment, they used an 18 inch diameter column and one and one-half inch Raschig rings. The height of the packing was varied. They concluded that liquid-film mass transfer coefficients and effective interfacial areas are the same for concurrent and countercurrent flow. This is not borne out by the work of Ufford (30) and Gianetto (12).

Gianetto, et.al. (12) measured effective interfacial area by gas absorption in the presence of variously fast chemical reactions in the liquid phase with known kinetics. They used concurrent gas-liquid flow through a packed bed. Under concurrent flow conditions, there are four main hydrodynamic regimes: Low gas and liquid velocities result in a gas continuous flow in which the behavior of the two phases is similar to that observed under countercurrent conditions when flow values are well below the loading point. An increase in either flow rate is followed by an increasingly evident interaction between the two phases, seen first as ripples on the surface of the liquid (rippled flow), then as annular liquid droplet pistons (pulsing flow), and lastly as a uniform suspension of minute droplets by the gas (spray flow).

The four regimes reflect changes in the hydrodynamic situation with different effects on interfacial areas and transfer coefficients.

Gianetto (12) measured interfacial areas for four different types of packing (six millimeter glass spheres, six millimeter glass and ceramic rings and six millimeter Berl saddles). During pulsing flow and spray flow in particular, interfacial area was mainly due to droplet formation. Effective interfacial area values in these regimes were correlated as a function of the dissipated energy and geometrical characteristic of the packing. They concluded that the concurrent packed columns offer a mass transfer efficiency that is considerably higher than that of conventional countercurrent columns. This is the result of their increased interfacial area, which may exceed the geometrical area, and increased transfer coefficients.

Gianetto (12) measured gas phase and liquid phase mass coefficients by means of a large series of experiments covering the absorption of NH_3 and desorption of O_2 with a controlling resistance in the gas phase and liquid phase respectively.

Shulman, et.al. (27) measured interfacial area and liquid-film mass transfer coefficient for different sizes of packing in countercurrent flow. They calculated effective interfacial area, a, from reliable sources of $k_G a$ data. The data of Fellinger for ammonia absorption in water were used. Then for values of k_L, the data of Sherwood and Holloway (26) were used. They measured $k_L a$ for different ceramic rings by desorption of slightly soluble gases from water. Shulman's data covered up to the loading point.

Richards, et.al. (23) measured interfacial area for one-half inch Raschig rings in a four inch internal diameter column. They operated the column countercurrently. They used different flow rates but the gas flow rate was not specified. They used absorption of carbon dioxide into catalyzed buffer solutions of carbonate-bicarbonate. Values of liquid-film mass transfer coefficients and interfacial areas for different flow rates from their work were plotted by Danckwerts and Sharma (9). The latter authors mentioned Mannford Doble's work with a carbon dioxide-air mixture as a gas phase to measure interfacial area and liquid-film mass transfer coefficients. Danckwerts and Sharma concluded that values of a and k_L are independent of gas flow rate as long as the loading point was not approached. Their data covered liquid rates up to 8000 lb/hr. $ft.^2$.

Puranik and Vogelphol (20) correlated data for effective

interfacial areas in an irrigated packed column. They took all available data for countercurrent operated packed column and correlated effective interfacial area as function of Reynolds number, superficial liquid velocity, total dry area of the packing, density of liquid and surface tension. They concluded that by using their correlations one can predict interfacial area within a range of $\pm$ 20 percent.

Onda, et.al. (16) measured liquid-side mass transfer coefficients. The physical absorption of gas by water in a tower packed with Raschig rings was measured. From values of $k_L a$, k_L was separated using a proportionality constant and wetted area.

Andrieu and Claudel (1) measured interfacial area in a packed column by the sulfite oxidation method. They observed that interfacial area varies with gas flow rate for a constant liquid flow rate.

Joosten and Danckwerts (13) investigated the effect of a chemical reaction on effective interfacial areas in gas absorption. They concluded that interfacial areas obtained with chemical reactions are higher than the interfacial areas obtained by physical absorption.

Onda (15) and Porter and Tepleman (19) investigated flow distribution in packed columns. They investigated wall flow effects. They concluded that packing heights should not be more than several diameters of the column, and wall flow effects decrease as flow of the liquid increases.

Because of the possible advantages of the concurrent packed bed system and the paucity of data available for concurrent flow, this study was undertaken to provide liquid-film mass transfer

coefficients, k_L, and effective interfacial areas for one-half inch packing using gas-liquid system.

C. PURPOSE OF THE INVESTIGATION

The experimentation of this investigation was designed to determine liquid-film mass transfer coefficients and effective interfacial areas for the absorption of carbon dioxide into carbonate-bicarbonate solution in a packed column operated in concurrent flow at high liquid and gas rates. Specifically, the purposes of the project are presented in the following discussion. A review of the literature was made in an effort to determine previous work covering concurrent flow, concurrent flow mass transfer systems, and countercurrent studies of carbon dioxide-carbonate-bicarbonate system. Experimental observations of liquid-film mass transfer coefficients and effective interfacial areas were made at high liquid rates for a concurrently operated packed column. Effects of high gas flow rates on liquid-film mass transfer coefficients and effective interfacial areas were also observed. A comparison of $(k_La)_{physical}$ and $(k_La)_{chemical}$ was made. By using two different heights of the packing, the wall effect was investigated. The purpose of this work is to contribute to the body of knowledge concerning gas absorption in packed beds by measuring rates of absorption and determining liquid-film mass transfer coefficients and effective interfacial areas.

D. SCOPE OF THE INVESTIGATION

The absorption of carbon dioxide into carbonate-bicarbonate

from a CO_2-air mixture was carried out. The composition of the CO_2-air mixture used was ten percent. The packed column was a 10.2 cm. I.D. Pyrex glass pipe packed with one-half inch Raschig rings. Two heights of packing were used--25.4 cm. and 91.44 cm. Gas velocities (superficial) ranged from 13.1 cm/sec to 56.5 cm/sec. Liquid velocities (superficial) ranged from 0.655 cm/sec to 2.65 cm/sec. The water used was city tap water. The temperature of the solution was kept within $\pm$ one degree of 25 degrees centigrade.

CHAPTER II

THEORY

At any point in the column the rate of absorption of the gas into the liquid per unit area of contact, R, times the interfacial area per unit packed volume, a, can be expressed in terms of concentration in the liquid phase by

$$Ra = Ek_L a(A^* - A^\circ) \tag{1}$$

Similarly in terms of concentrations in the gas phase by

$$Ra = k_G a(p - p_i) \tag{2}$$

The area factor, a, usually is associated with both sides of the expression because it can rarely be obtained. If Henry's law is applicable $p_i = HeA^*$ and the rate expression can be written:

$$Ra = k_G a(p - HeA^*) = Ek_L a(\frac{p}{He} - A^\circ) \tag{3}$$

In terms of overall resistances, the rate expressions are:

$$Ra = K_G a(p - p^*) \tag{4}$$

$$Ra = EK_L a(A^* - A^\circ) \tag{5}$$

From the equilibrium curve,

$$p - p^* = (p - p_i) + (p_i - p^*) \tag{6}$$

From Henry's law,

$$p - p^* = (p - p_i) + He(A^* - A^\circ) \tag{7}$$

From equations (7), (4), and (1), one can get

$$\frac{1}{K_G a} = \frac{1}{k_G a} + \frac{He}{Ek_L a} \tag{8}$$

Similarly, one can get

$$\frac{1}{EK_L a} = \frac{1}{Ek_L a} + \frac{1}{Hek_G a} \tag{9}$$

When the Henry's law constant is very large (i.e., the gas is slightly soluble) as is the case in the system of this work, it can be seen that the second term in equation (9) becomes small. In this case the liquid-film resistance is controlling the absorption process

$$\frac{1}{K_L a} \approx \frac{1}{k_L a} \tag{10}$$

The overall coefficient is nearly equal to the individual liquid phase coefficient.

All methods for predicting rates of absorption into reacting

liquid in industrial equipment under specified conditions require a separate knowledge of k_L, the liquid film mass transfer coefficient, and a, the effective interfacial area, in the specified packing under specified operating conditions. The quantity of $k_L a$ can easily be found by absorption measurements, by taking steps to eliminate gas-side resistance.

A number of methods have been used for estimating a. In this investigation Danckwerts (7) model was used.

The following is the derivation for liquid-film resistance and interfacial area. The dissolved gas A reacts with a reactant B,

$$A + B \rightarrow P$$

The concentrations of B and A are governed by the following equations: (In the following treatment, the diffusitivites of A and B are taken to be equal.)

$$D_A \frac{\partial^2 b}{\partial x^2} = \frac{\partial b}{\partial t} + k_1 c \qquad (11)$$

with

$$b = B^\circ \qquad x > 0 \qquad t = 0$$

$$b = B^\circ \qquad x = \infty \qquad t > 0$$

$$\frac{\partial b}{\partial x} = 0 \qquad x = 0 \qquad t > 0$$

$$D_A \frac{\partial^2 c}{\partial x^2} = \frac{\partial c}{\partial t} + k_1 c \qquad (12)$$

with

$c = 0 \quad x > 0 \quad t = 0$

$c = A^* \quad x = 0 \quad t > 0$

$c = 0 \quad x = \infty \quad t > 0$

Transferring equation (12) into Laplace form, one can get

$$D_A \frac{d^2\bar{c}}{dx^2} = \bar{c}(k_1 + s) \tag{13}$$

with

$\bar{c} = A^* \quad x = 0$

$\bar{c} = 0 \quad x = \infty$

where

$$\bar{c} = s \int_0^\infty c\, e^{-s\theta}\, d\theta \tag{14}$$

The solution of equation (13) is

$$\bar{c} = A^* \exp\left(-\frac{xk_L}{D_A}\sqrt{\left(1 + \frac{D_A k_1}{k_L^2}\right)}\right) \tag{15}$$

Transferring equation (11) into Laplace form, one can get

$$D_A \frac{d^2\bar{b}}{dx^2} = s(\bar{b} - B^\circ) + k_1\bar{c} \tag{16}$$

Inserting the value of $\bar{c}$ from equation (15) and putting

$$\gamma = \frac{k_L}{D_A}\sqrt{1 + \frac{D_A k_1}{k_L^2}} \tag{17}$$

$$D_A \frac{d^2\bar{b}}{dx^2} = s(\bar{b} - B^\circ) + k_1 A^* e^{-\gamma x} \tag{18}$$

with

$$\bar{b} = 0 \qquad x = \infty$$

$$\frac{d\bar{b}}{dx} = 0 \qquad x = 0$$

The solution of $\bar{b}$ is

$$\bar{b} = B^\circ - \frac{k_1 A^*}{\gamma^2 D_A - s}\sqrt{\frac{D_A}{s}} \quad \exp\left(-x\sqrt{\frac{s}{D_A}}\right)$$

$$+ \frac{k_1 A^*}{\gamma^2 D_A - s} \exp(-\gamma x) \tag{19}$$

whence

$$(\bar{b})_{x=0} = B^\circ + \frac{k_1 A^* \left(1 - \gamma\sqrt{\frac{D_A}{s}}\right)}{\gamma^2 D_A - s} \tag{20}$$

Since $k_L = \sqrt{D_A s}$ we have a discrepancy between B° and $\bar{b}$ at $x = 0$

$$\frac{B^\circ - (\bar{b})_{x=0}}{B^\circ} = \frac{A^*}{B^\circ}\left[\sqrt{1 + \frac{D_A k_1}{k_L 2}} - 1\right] \tag{21}$$

If this discrepancy is small at this point then the reaction can be treated as a pseudo-first-order reaction. For the reaction to be a pseudo-first-order reaction the following condition must be satisfied:

$$\sqrt{1 + \frac{D_A k_1}{k_L^2}} - 1 \ll \frac{B^\circ}{A^*} \tag{22}$$

In Danckwerts' model, the average rate of absorption per unit volume of packing is given by

$$Ra = {}_o\int^\infty R_1 a \psi(t)\, dt \tag{23}$$

Applying the Laplace transportation on equation (23), one can get

$$Ra = s \int_o^\infty R_1 a\, e^{-s\theta}\, d\theta \tag{24}$$

The rate of absorption of gas at any time is given by

$$R_1 a = -D_A \left(\frac{\partial c}{\partial x}\right)_{x=0} \tag{25}$$

Putting equation (25) into equation (24), one can get

$$Ra = sa\, {}_o\int^\infty - D_A \left(\frac{\partial c}{\partial x}\right)_{x=0} e^{-s\theta}\, d\theta \tag{26}$$

$$Ra = -D_A a \left(\frac{d}{dx}\, s \int_0^{\infty} c\, e^{-s\theta}\, d\theta\right)_{x=0} \qquad (27)$$

Inserting equation (14) into equation (27), one can get

$$Ra = -D_A a \left(\frac{d\bar{c}}{dx}\right)_{x=0} \qquad (28)$$

Getting $\left(\frac{d\bar{c}}{dx}\right)_{x=0}$ from equation (15) and putting it into equation (28), one can get

$$Ra = k_L\, a\, A^* \sqrt{1 + \frac{D_A k_1}{k_L^2}} \qquad (29)$$

Rearranging equation (29), the rate of absorption will then be

$$Ra = a\, A^* \left(\sqrt{D_A k_1 + k_L^2}\right) \qquad (30)$$

where $k_1 = k_L\,(Cat)$.

The experimental method is based on equation (30). The concentration of catalyst is varied while all the variables are held constant and the rates of absorption are measured for different catalyst concentrations. Then a plot is made of $(Ra)^2$ against k_1, and a straight line should result with slope $(aA^*)^2 D_A$ and intercept $(k_L aA^*)^2$. By knowing A^* and D_A, one can calculate k_L and a separately. This method has been used by Richards, et.al. (23) and by Danckwerts and Gillham (8).

The CO_2-air-carbonate-bicarbonate system was chosen in this

project. The kinetics of the reaction of CO_2 and carbonate-bicarbonate has been investigated by Roberts and Danckwerts (24). They have concluded that the reaction between CO_2 and carbonate-bicarbonate buffer solution is a pseudo-first-order and the rate of absorption can be increased by using a catalyst such as hypochlorite or arsenite.

The CO_2-air carbonate-bicarbonate system can be described as a mass transfer process where CO_2 is transferred from a moving gaseous phase CO_2-air mixture into concurrently moving liquid (carbonate-bicarbonate) in which it is slightly soluble and reacts with carbonate, so that the concentration of the gas in the liquid phase increases as the two phases move through the packed bed.

The following reactions take place as CO_2 is absorbed in the carbonate-bicarbonate solution,

$$CO_2 + Na_2CO_3 + H_2O \rightarrow 2NaHCO_3 \qquad (31)$$

Reaction (31) may be written more realistically in ionic terms,

$$CO_2 + CO_3^{--} + H_2O \rightarrow 2HCO_3^- \qquad (32)$$

Reaction (32) is made up by a sequence of reactions in a weakly alkaline solution,

$$CO_2 + H_2O \rightarrow HCO_3^- + H^+ \qquad (33)$$

$$CO_2 + OH^- \rightarrow HCO_3^- + H^+ \quad (33)$$

Both reactions (33) and (34) are followed by an instantaneous reaction leading to the overall results expressed by reaction (32),

$$CO_3^{--} + H^+ \rightarrow HCO_3^- \quad (35)$$

$$CO_3^{--} + H_2O \rightarrow HCO_3^- + OH^- \quad (36)$$

Reactions (35) and (36) are just proton exchange, therefore these reactions are instantaneous.

The rate determining step, reaction (33) has a rate constant of 0.0257 sec^{-1} at 25°C. However, the reaction can be catalyzed by a variety of agents; hypochlorite was used as a catalyst for speeding the absorption of CO_2. Catalyst concentration was varied from 0 - 0.035M.

Taveres Da Silva and Danckwerts (28) have shown that the catalytic rate constant for hypochlorite at 25°C is

$$k_c = 920 + 5750\ (CO_3^{--})\ \text{l/gm moles sec} \quad (37)$$

where (CO_3^{--}) is in gm moles/liter.

CHAPTER III

EXPERIMENTAL EQUIPMENT AND PROCEDURE

A. DETAILS OF THE EQUIPMENT

The packed bed in which the absorption process was carried out was made by packing a length of four inch I.D. pyrex glass pipe with one-half inch Raschig rings. Two lengths of packing were used, a 25.4 cm. and a 91.44 cm. section. The packed column was identical to one described by Ufford (30). A closed top was designed and constructed to hold the pressure and is shown in Figure 1, along with other details of the column. The gas and liquid streams were fed into the top of the column. The liquid entered from a one and one-fourth inch pipe emptying into the entrance section and was distributed through four holes one-half inch in diameter located symmetrically about the center of a stainless steel distribution plate 0.034 inch thick. The gas tube (one-eighth inch I.D.) released the gas below the plate and just above the packing. A pressure top was inserted into the top, and a one-eighth inch tube was extended to a point just below the distribution plate. Later, for the higher flow rates 5/32 inch I.D. gas tube was used.

Figure 2 is a diagram of the entire experimental setup. First the solution of desired molarity was made in the mixing tank. Then it was pumped up into the constant head storage tank. From there liquid was fed to the top of the packed column. The liquid flow

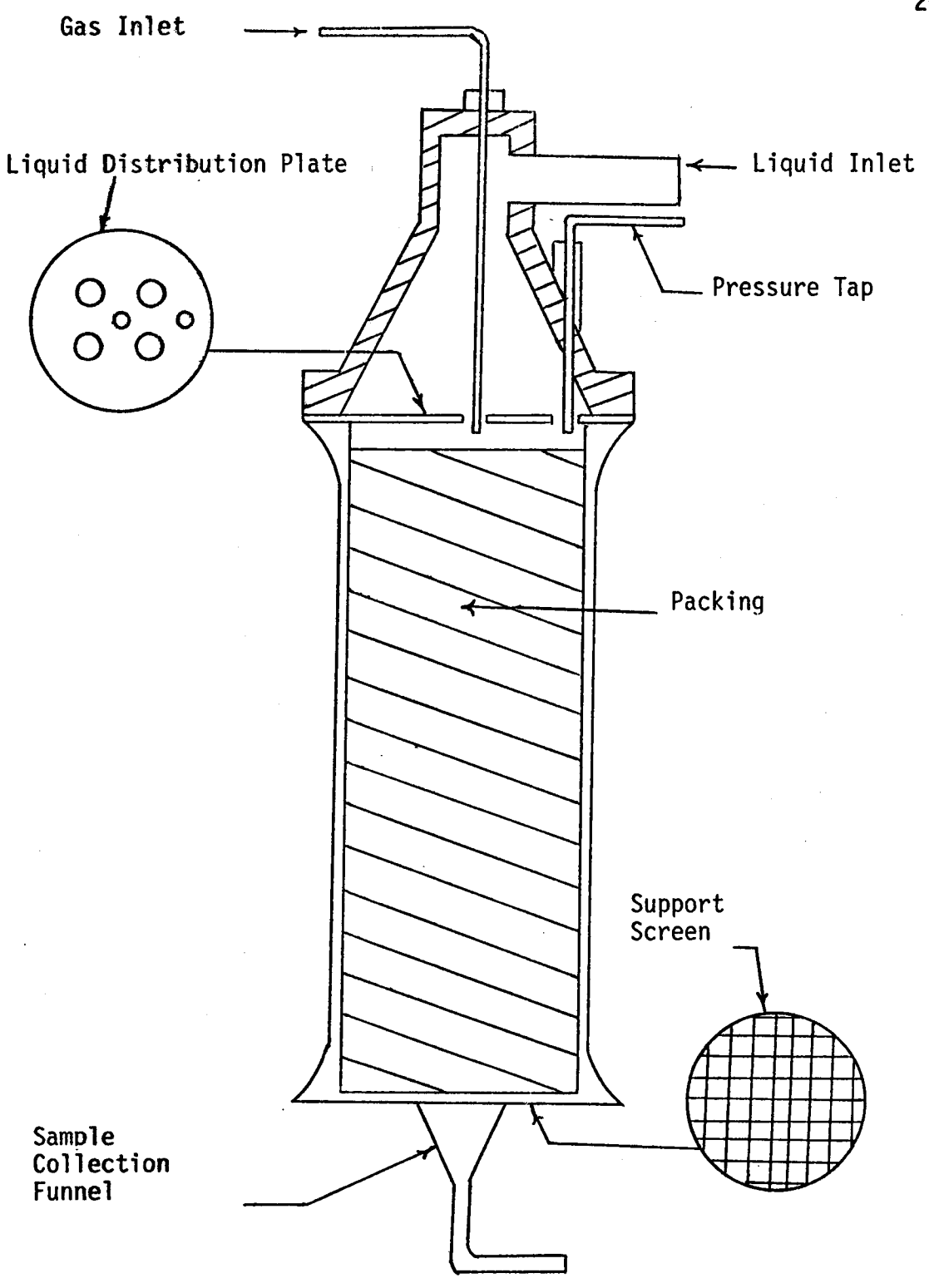


Figure 1. Details of the Packed Column

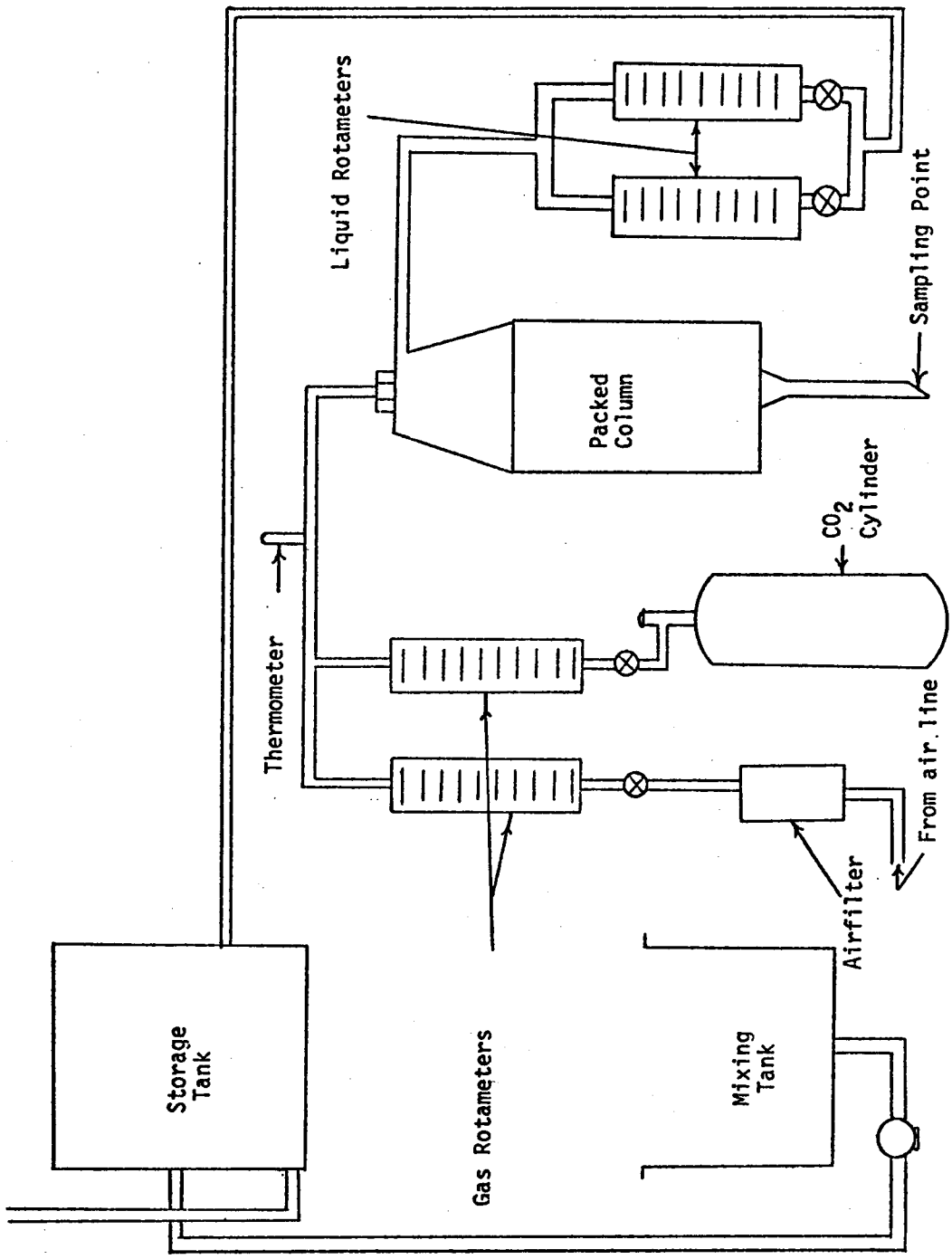


Figure 2. Diagram of Experimental System

rates were measured by using a Fisher and Porter rotameter. The rotameter was calibrated using a 1000 (±) pound Toledo scale with a barrel and stop watch. The calibration curve is shown in Figure 18 (see Appendix B).

The gas feeding system mixed two gas streams, an air stream and a carbon dioxide stream, before feeding the mixture into the packed column. The air was taken from the laboratory supply line and it was fed through the air-oil filter. The air flow was measured by using two Fisher and Porter rotameters to cover the range required. Both rotameters were calibrated by using an 800 liters/hr. capacity wet test meter. The carbon dioxide was fed from a pressurized cylinder through a regulator. The CO_2 flow was measured by using another Fisher and Porter rotameter. This rotameter was also calibrated by using an 800 liters/hr. capacity wet test meter. The air and carbon dioxide streams were mixed together and temperature was measured prior to feeding the stream at the top of the tower by using thermometer. The temperature of the gas stream was 25°C (± one degree Centigrade) throughout the experiments.

The data were taken by using one-half inch Raschig rings as a packing material. Porter and Tepleman (19) suggest that the ratio of the nominal packing size to the tower diameter be less than 1:10 to 1:8 to make the wall effect small. With one-half inch Raschig rings the ratio is 1:8. The effect of too large a packing is to cause liquid channelling to the column wall. This wall effect causes deviation from the ideal homogeneous model used to derive the liquid-film mass transfer coefficient, k_L, and effective

interfacial area, a. Both Porter and Tepleman (19) and Danckwerts and Gillham (8) have examined the height effect and they have revealed that height of the column should not exceed a few column diameters in order to avoid significantly adverse effects.

The important details of the packed column are shown in Figure 1. At the bottom of the column the sample was collected by a small funnel located just below the packing supported screen. The temperature of the entering and effluent streams was measured by using thermometers.

B. EXPERIMENTAL PROCEDURE

The experiment involved the measurement of the concentration of absorbed carbon dioxide in the effluent liquid stream from the column by a standard quantitative method as outlined in several sources (11, 25). Standardized solutions of hydrochloric acid and sodium hydroxide were used. Both solutions were near 0.03 molar. The solutions were mixed from laboratory reagents. Hydrochloric acid was standardized by titration with sodium carbonate using a potentiometer technique. The sodium hydroxide was standardized by titrating with standardized hydrochloric acid.

To determine the carbonate content of the sample, a five milliliter of sample was pipetted into 50 millileters of distilled water which was previously pipetted into a 250 milliliter beaker. Then by using a constant pH recorder and a diffusion pump, hydrochloric acid was added with a constant flow of five milliliter/minute and the pH change was recorded on graph paper. An example curve is shown

in Figure 3. The point of inflection of a curve was found and from that amount of hydrochloric acid required for the first equivalent point was calculated the molarity of sodium carbonate.

To determine bicarbonate content of the sample, five milliliters of sample was pipetted into a 250 millileter Erlenmeyer flask. Then 50 milliliters of sodium hydroxide was added. Immediately ten milliliters of ten percent barium chloride and two drops of phenolphthalein were added. The excess of sodium hydroxide was titrated with 0.03M HCl solution to the disappearance of the pink color. From this molarity of sodium bicarbonate was also calculated. This was done for the sample from the top of the column and also from the bottom of the column. From the change in molarity the rate of absorption of carbon dioxide was calculated.

A day in the laboratory was begun by flushing the column with water for several minutes. Then a solution of 0.207M Na_2CO_3 and 0.215M $NaHCO_3$ was made in the mixing tank. When catalyst was needed, the catalyst was added in the required amount. The catalyst concentration was varied from 0 - 0.035M. Sodium hypochlorite was used as catalyst. The solution was then pumped into a constant head tank. Before making a run, atmospheric pressure and room temperature were noted. When the run was started, a sample from the top of the column was taken. After ten minutes of liquid and gas flow, an effluent sample from the bottom of the column was taken. To make sure it reached steady state, another sample was taken after five minutes.

A total of 51 runs were made, with three to four catalyst

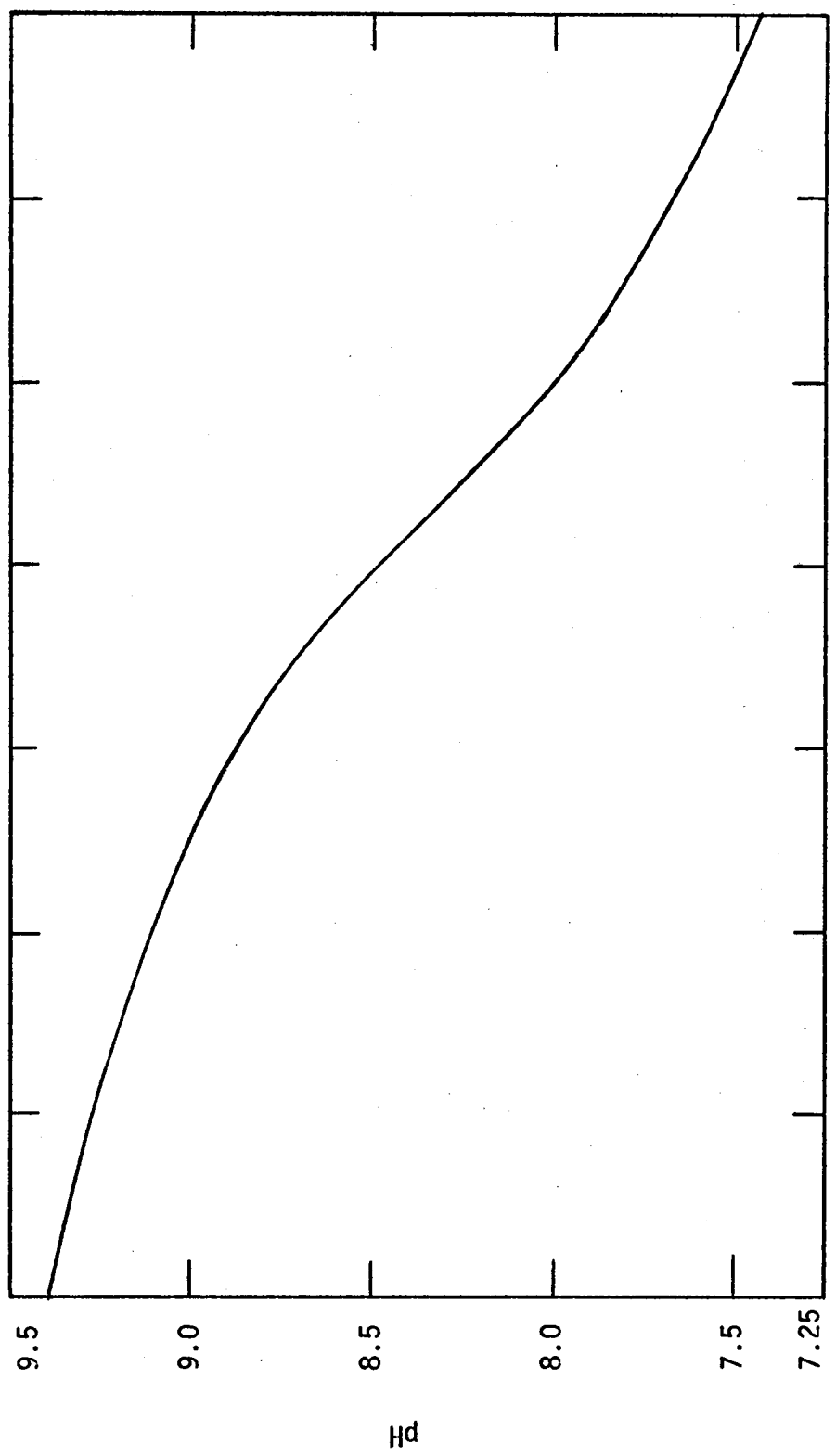


Figure 3. Diagram of pH Versus Amount of HCl

concentrations for each liquid and gas rate. These runs consumed 240 pounds of Na_2CO_3, 200 pounds of $NaHCO_3$, and 87 liters of sodium hypochlorite.

CHAPTER IV

RESULTS AND DISCUSSION

A. RESULTS OF LIQUID-FILM MASS TRANSFER COEFFICIENTS AND EFFECTIVE INTERFACIAL AREA

As previously stated in the experiment procedure, samples of each run were titrated with hydrochloric acid and sodium hydroxide. From the analysis the molarity of sodium carbonate was found for the samples from the top of the column and from the bottom of the column. Rotameter settings were converted to flow rates. The original absorption rate data is reproduced in Tables 1, 2, 3 and 4 (Appendix C). The calculation results are given in Tables 7 and 8 (Appendix D). The plots of $[Ra]^2$ against k_1 are shown in Figures 4, 5, 6, and 7. The slope and intercept of each line are given in Tables 5 and 6 (Appendix D).

Liquid-film mass transfer coefficients and effective interfacial areas were measured for gas rates ranging from 13.1 cm/sec to 56.5 cm/sec and for liquid rates up to 2.65 cm/sec. Effective interfacial area varies from 2.28 cm^2/cm^3 to 3.54 cm^2/cm^3 and the liquid-film mass transfer coefficient, k_L, varies from 11.7×10^{-3} cm/sec to 26.85×10^{-3} cm/sec. The effect of liquid rate on interfacial area is shown in Figure 8 and effect of gas rate is shown in Figure 10. Similar plots for k_L are shown in Figures 9 and 11. All these graphs were drawn on log-log paper because it was found in the literature that values of interfacial areas and k_L sometimes can be represented by a straight

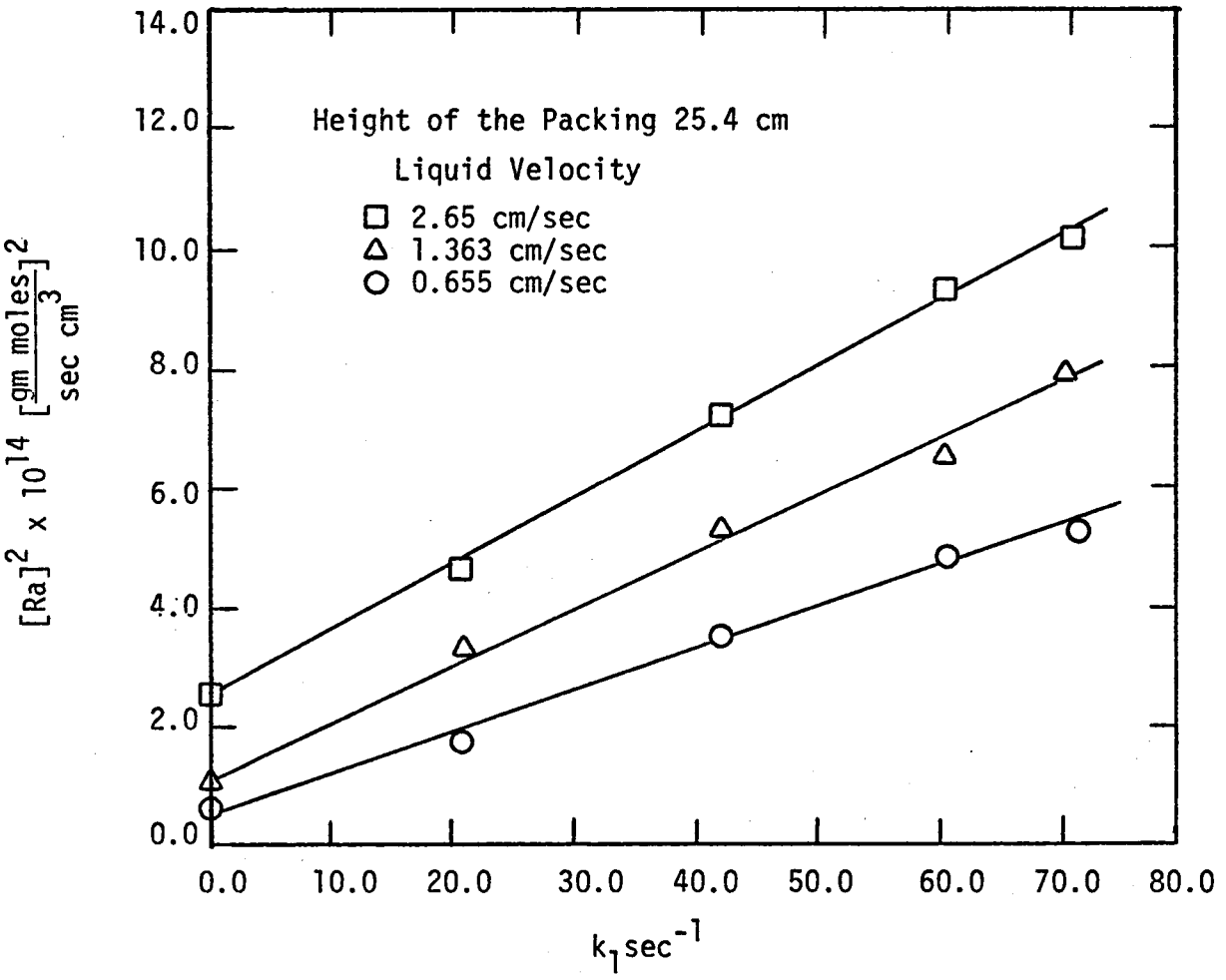


Figure 4. Absorption into Solutions Containing Hypochlorite in a Packed Column with the Gas Velocity 13.1 cm/sec

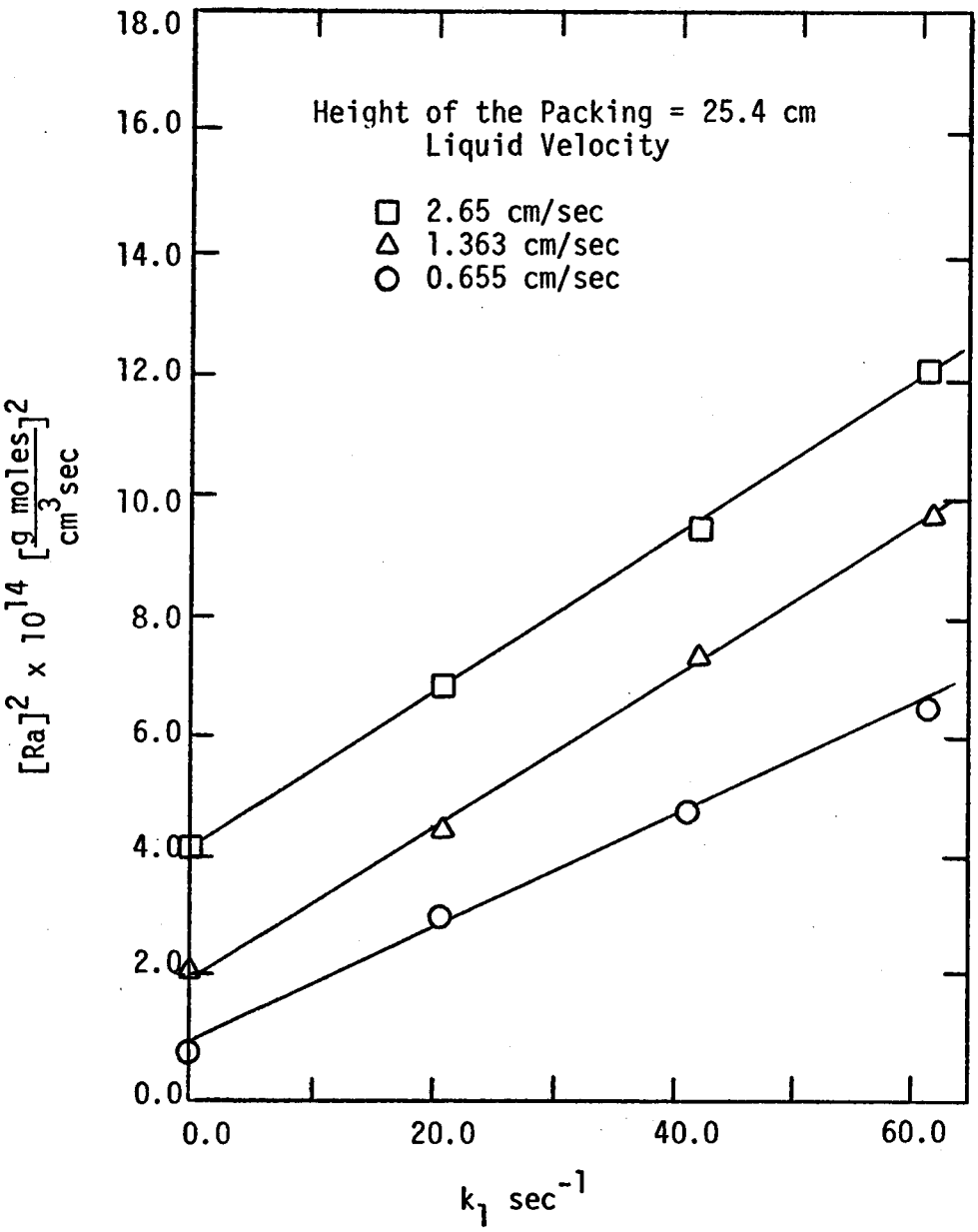


Figure 5. Absorption into Solutions Containing Hypochlorite in a Packed Column with the Gas Velocity 28.25 cm/sec

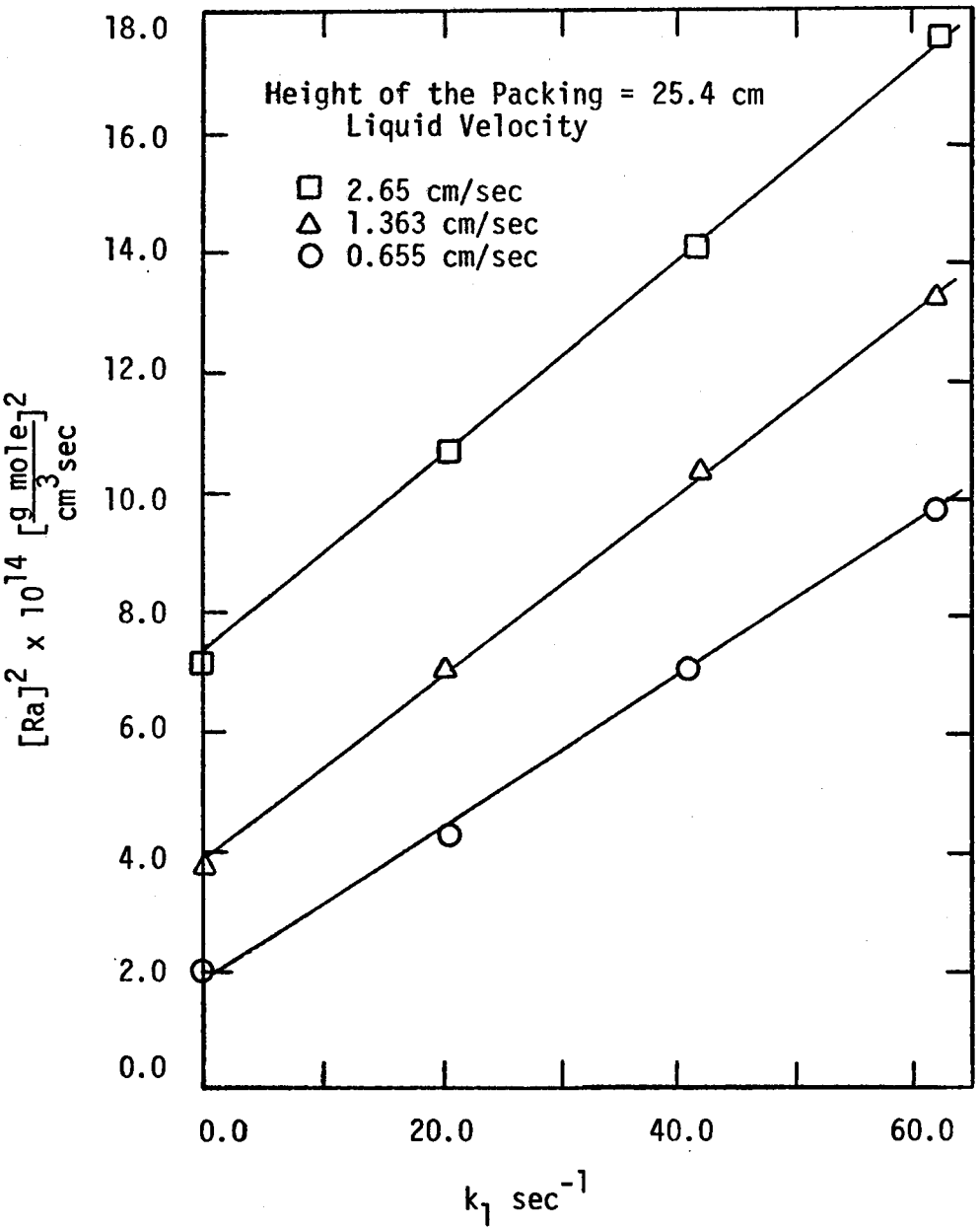


Figure 6. Absorption into Solutions Containing Hypochlorite in a Packed Column with the Gas Velocity 56.5 cm/sec

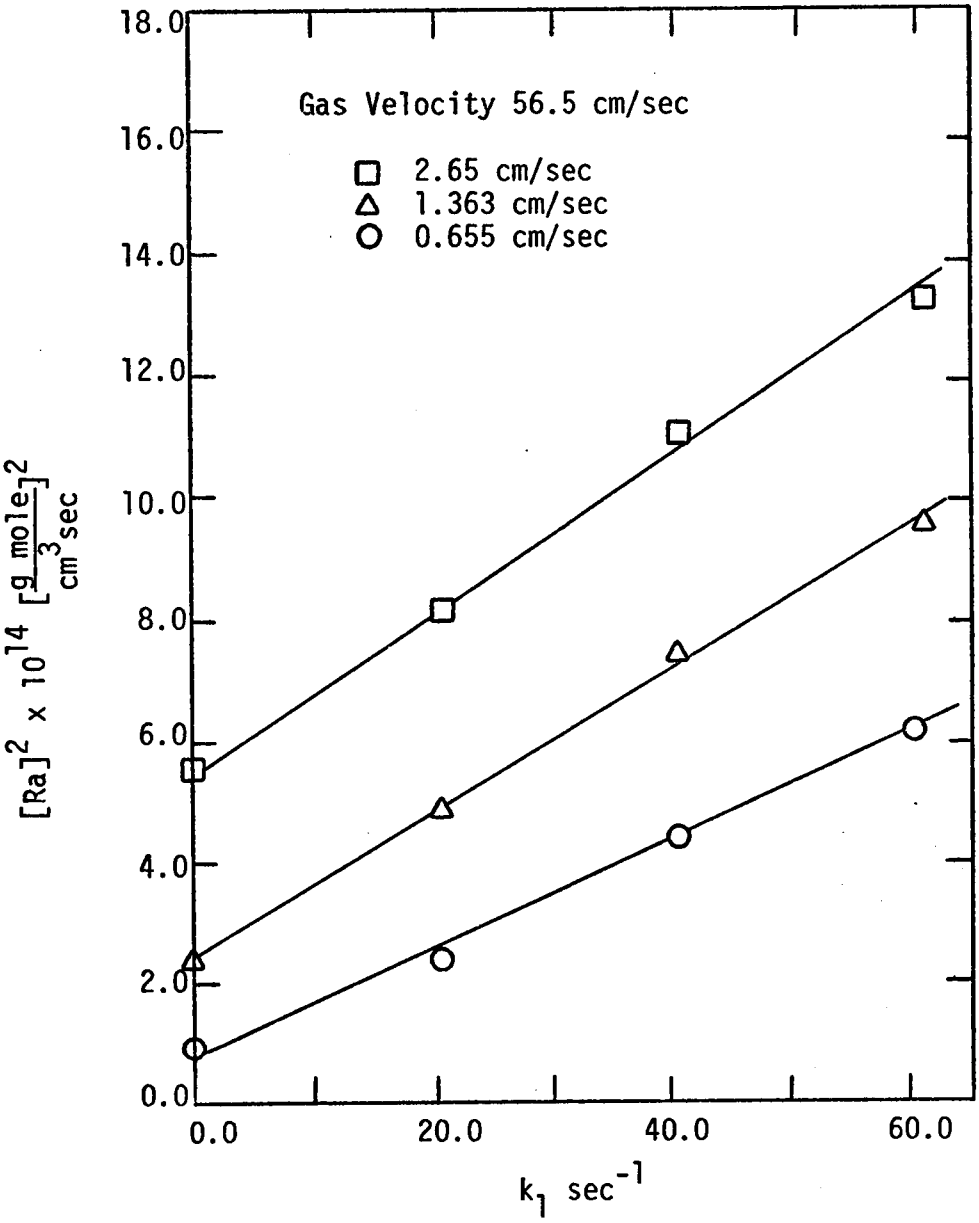


Figure 7. Absorption into Solutions Containing Hypochlorite in a Packed Column 91.44 cm in Height

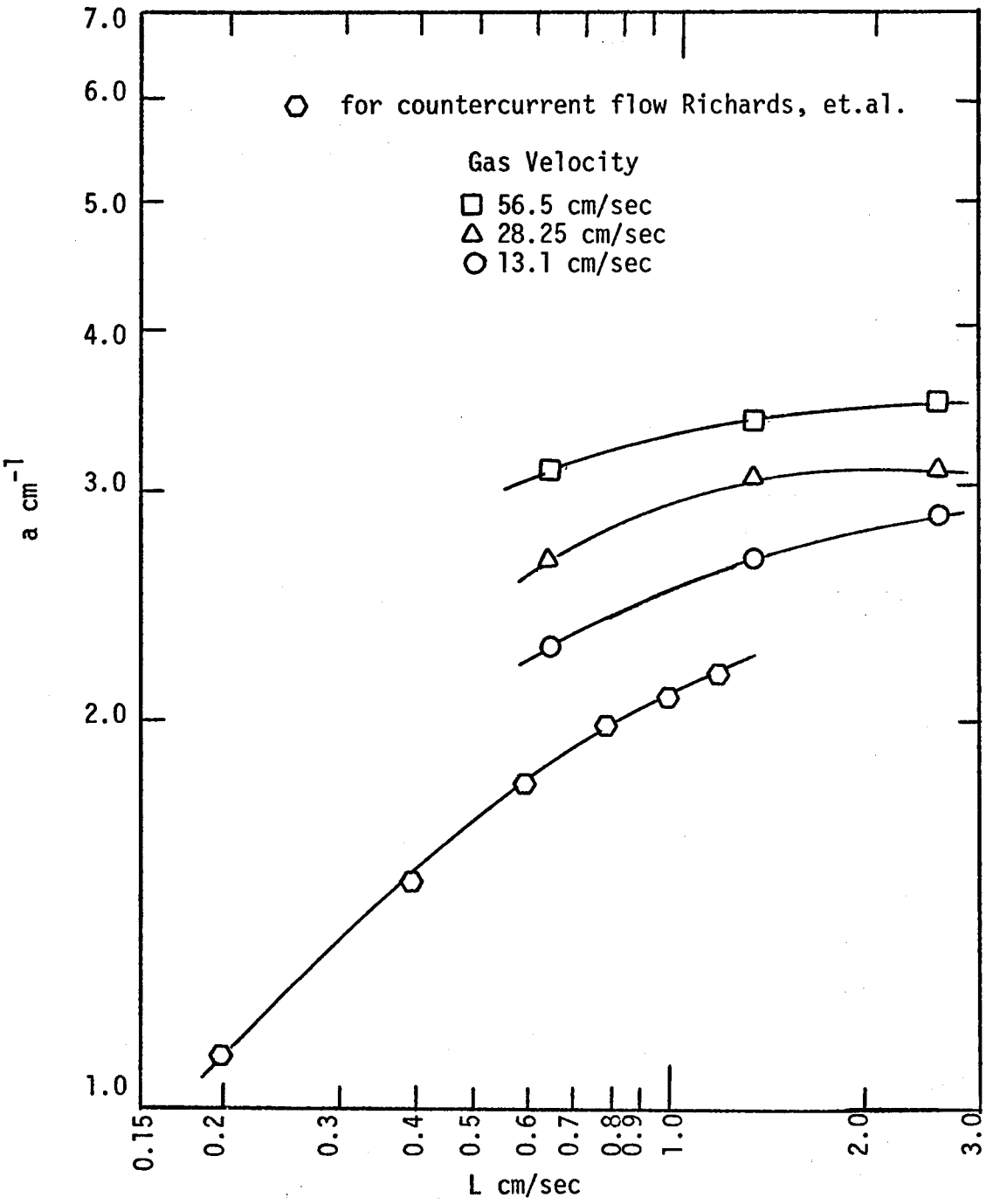


Figure 8. Effect of Liquid Superficial Velocity on Effective Interfacial Area

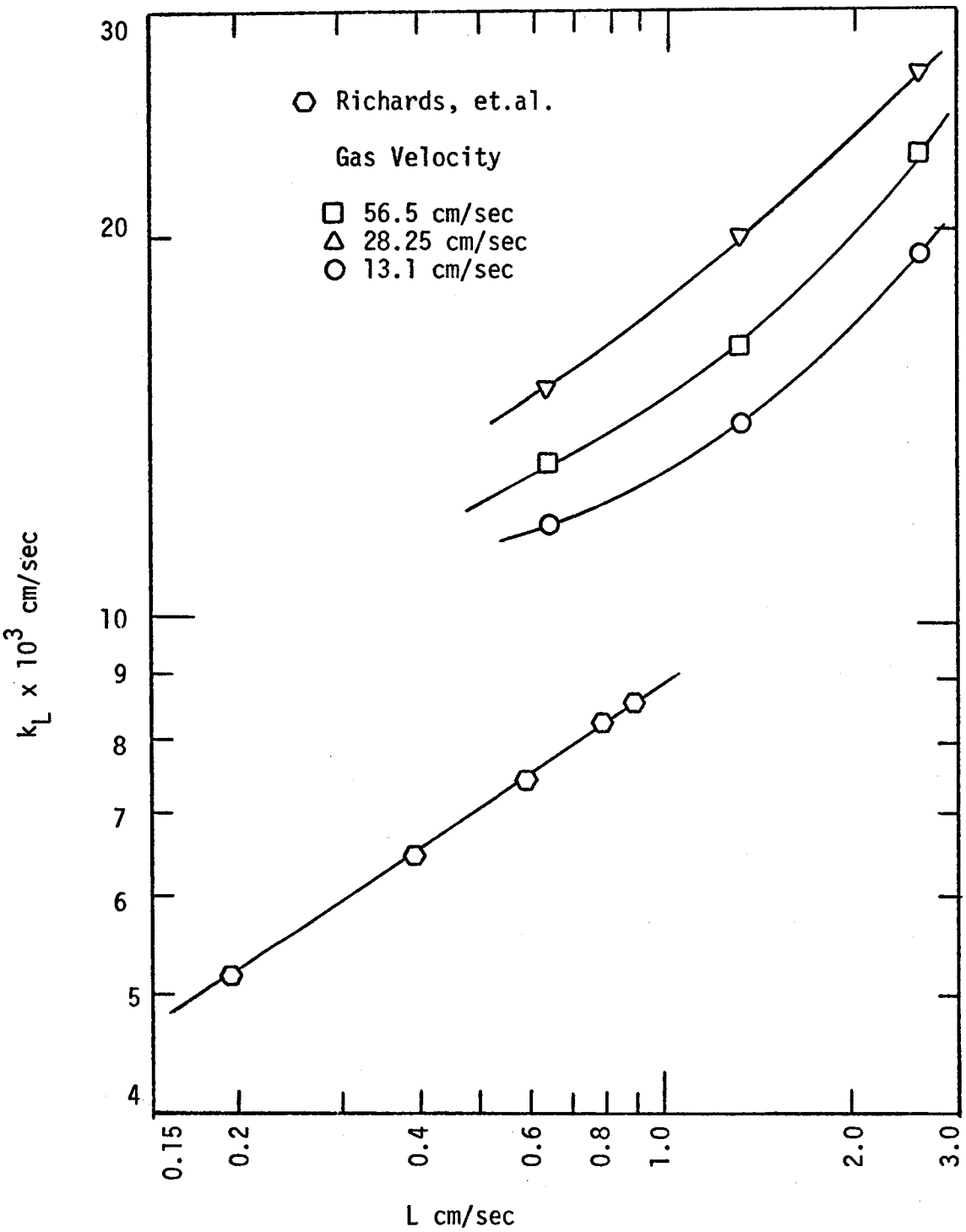


Figure 9. Effect of Liquid Superficial Velocity on Liquid-Film Mass Transfer Coefficient, k_L

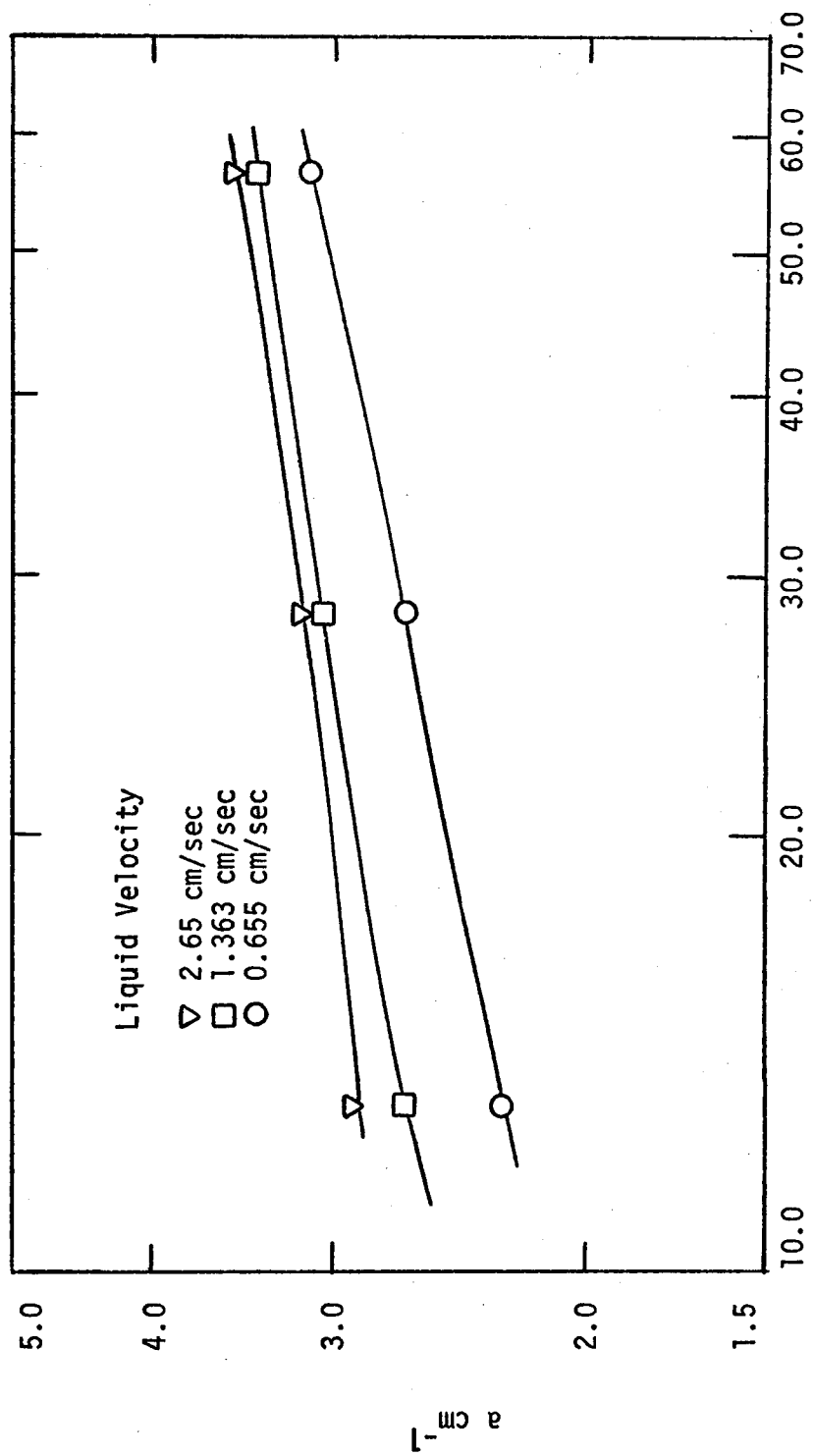


Figure 10. Effect of Gas Superficial Velocity on Effective Interfacial Area

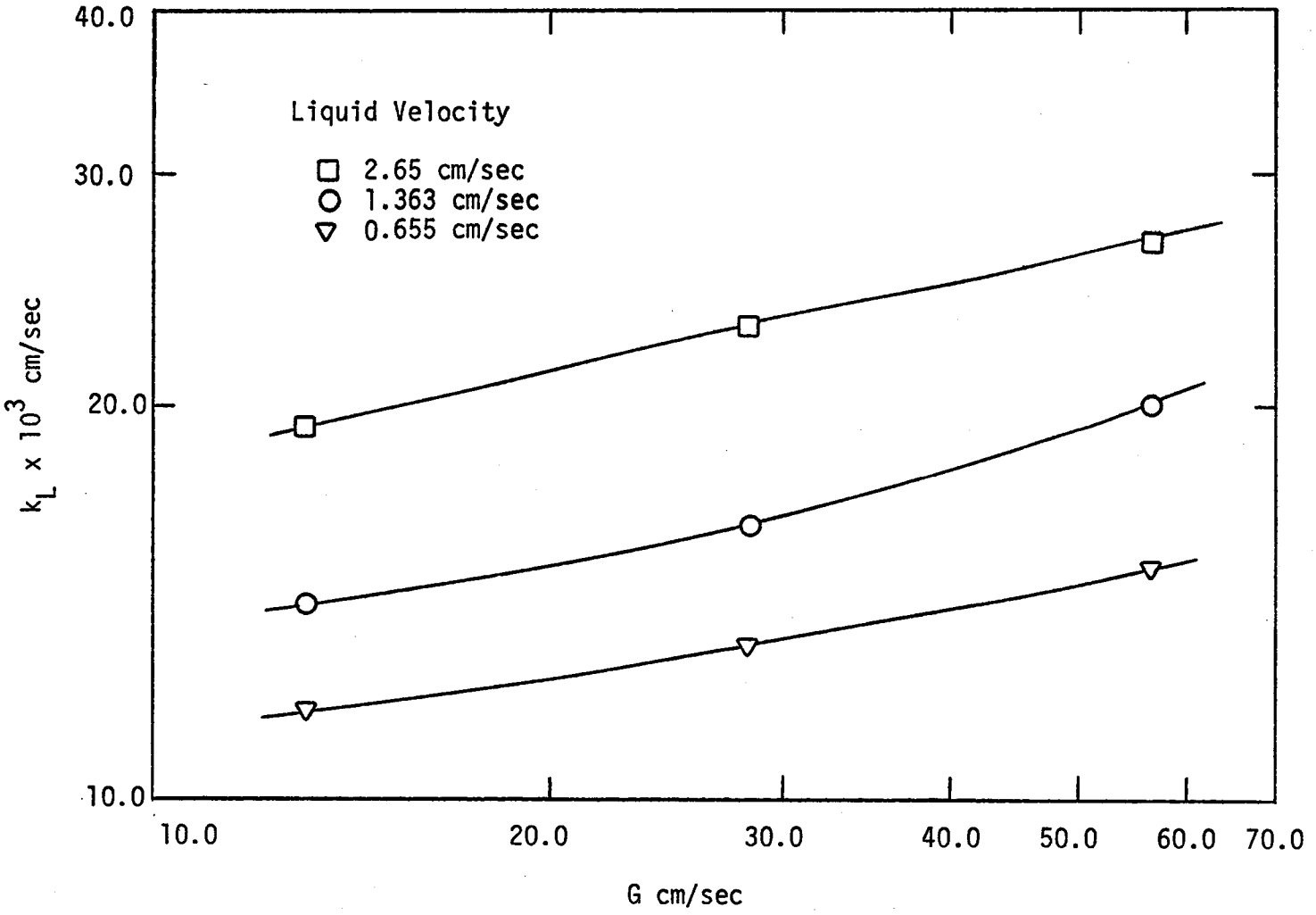


Figure 11. Effect of Gas Superficial Velocity on Liquid-Film Mass Transfer Coefficient, k_L

line. In the present work it was not observed.

The effective interfacial area increases with increasing gas rate. On log-log paper, the plot of effective interfacial area against gas flow rate gives almost a straight line. The effect of gas rate is to increase area by a factor of about 1.3 as the gas velocity increases from 13.1 cm/sec to 56.5 cm/sec.

The effective interfacial area increases with increasing liquid rate, but it tends to taper off. On log-log paper curves of effective interfacial area against liquid flow rates are concave downward. The effect of the liquid rate is to increase a by a factor of about 1.2 as the liquid velocity increases from 0.655 cm/sec to 2.65 cm/sec.

The effect of gas velocity on liquid-film mass transfer coefficients, k_L, is shown in Figure 11. Liquid-film mass transfer coefficient increases by a factor of 1.3 as gas rate increases from 13.1 cm/sec to 56.5 cm/sec. On log-log paper, liquid-film mass transfer coefficient plotted against gas velocity gives almost a straight line.

The effect of liquid velocity on liquid-film mass transfer coefficients is shown in Figure 9. Liquid-film mass transfer coefficients are moderately affected by liquid rate. Liquid-film mass transfer coefficient increases by a factor of 1.7 as liquid rate increases from 0.655 cm/sec to 2.65 cm/sec. On log-log paper, liquid-film mass transfer coefficients plotted against liquid rates. Curves were concave upward.

B. COMPARISON OF EFFECTIVE INTERFACIAL AREA AND LIQUID-FILM MASS TRANSFER COEFFICIENT WITH LITERATURE

In attempting to compare the results with those of previous investigations, no direct comparisons to values obtained in the same system in concurrent flow or to general correlations for concurrent flow could be made, for none were found in the literature. The mass transfer coefficients, k_L, and interfacial areas, a, obtained in the present investigation could be compared to the results obtained for different packings in concurrent flow and the same system in countercurrent flow.

Gianetto, et.al. (12) measured interfacial area by gas absorption in the presence of variously fast chemical reactions in the liquid-phase with known kinetics. They concluded that concurrent packed columns offer a mass transfer efficiency that is considerably higher than that of conventional countercurrent columns. This is the result of their increased interfacial area, which may exceed the geometrical area, and increased transfer coefficients. In the present work, interfacial areas are higher than those found for countercurrent flow for the same system, but values do not exceed the geometrical area.

Gianetto, et.al. (12) measured liquid-film mass transfer coefficients in the packed column for concurrent gas-liquid flow. The liquid-film mass transfer coefficients were studied by means of oxygen desorption with air from a 2N NaOH solution. They concluded that $k_L a$ increases 40 fold for approximately 15 fold increases in liquid velocity. In the case of k_L, these increments were obviously

less, although their magnitude nevertheless shows the notable efficiency of concurrent contact when the controlling resistance is in the liquid-phase. Their results with those of Danckwerts and Sharma (9) indicate that concurrent values of k_L are as much as ten times greater than those obtained in countercurrent columns under normal conditions.

The present work does not show the same trend as the Gianetto results with respect to the liquid rate effect on $k_L a$. Gianetto measured k_L and a for a different size of packing than the one used in the present work. Gianetto used six millimeter Raschig rings whereas in the present work 12.7 millimeter Raschig rings were used. They used gas flow rates from 38 cm/sec to 222 cm/sec and liquid rates from 0.3 cm/sec to 4.0 cm/sec. In the present work $k_L a$ increased by a factor of 1.7 for a 4.3 factor increase of gas flow rate and increased by a factor of 2.0 for a 4.0 factor increase of liquid flow rates.

Danckwerts (6) measured interfacial areas for one and one-half inch ceramic Raschig rings. They used countercurrent flow. Their results suggested that the value of specific interfacial area, a, levels off at something over a value of 1.4 cm^{-1} at higher liquid flow rates. This is somewhat higher than the geometrical surface area of the packing, suggesting that at higher flow rates not only is most of the surface of the packing effectively irrigated, but that drops may be falling through the gas as well. They revealed from Mannford Doble's work that gas velocity does not influence the interfacial area until the loading point is reached.

The maximum gas rate used in the present investigation is 56.5 cm/sec. For 12.7 millimeter Raschig rings the predicted liquid loading rate in countercurrent operation is 0.26 cm/sec. The flow rates in this investigation go far beyond those possible in countercurrent flow. Shulman (27) measured effective interfacial area, a, and liquid-film mass transfer coefficient, k_L, up to the loading point. They concluded that the effective interfacial area increases with increasing liquid rate and is fairly independent of gas rate which agrees with Danckwerts and Sharma (9) conclusion.

Richards, Ratcliff and Danckwerts (23) measured interfacial area for countercurrent flow in the packed column for one-half inch (12.7 millimeter) Raschig rings. A comparison of their results with the present work is shown in Figures 8, 9, and 12. Effective interfacial areas for countercurrent gas absorption are less by a factor of about 0.8 than for concurrent gas absorption, at a liquid rate of 0.655 cm/sec and at the lowest gas rate of 13.1 cm/sec, to a factor of about 0.6 at the highest gas rate of 56.5 cm/sec. Richards did not find any effect of gas velocity on the interfacial areas. In comparison with the present results, liquid-film mass transfer coefficients, k_L, for concurrent gas absorption are higher by factors of about 2.0 than for countercurrent gas absorption in contrast to the factor of up to ten found by Gianetto. Richards, et.al. used liquid flow rates far below the loading point. They did not reveal the gas flow rates used.

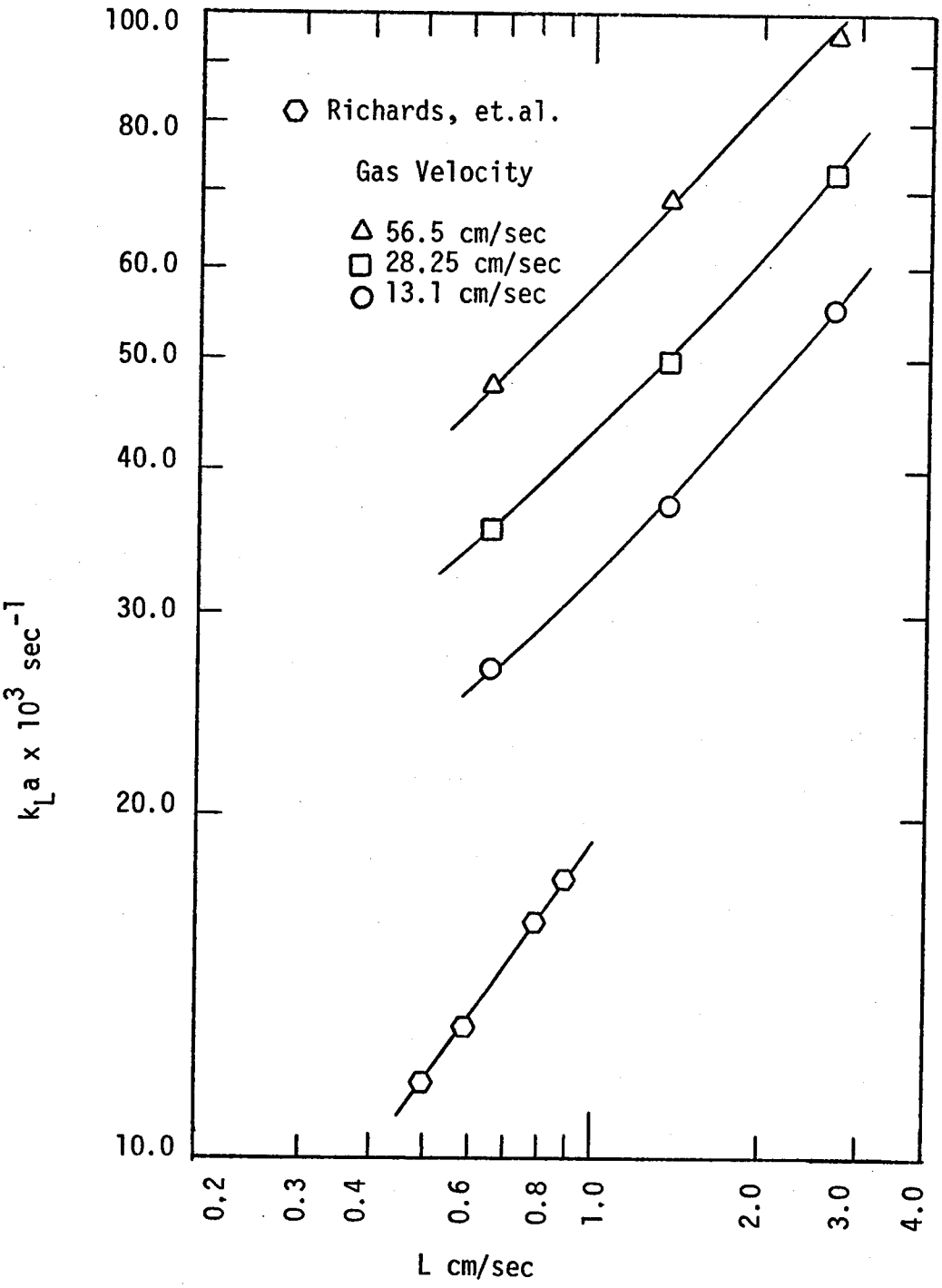


Figure 12. Effect of Liquid Superficial Velocity on Liquid-Phase Mass Transfer Coefficient, $k_L a$

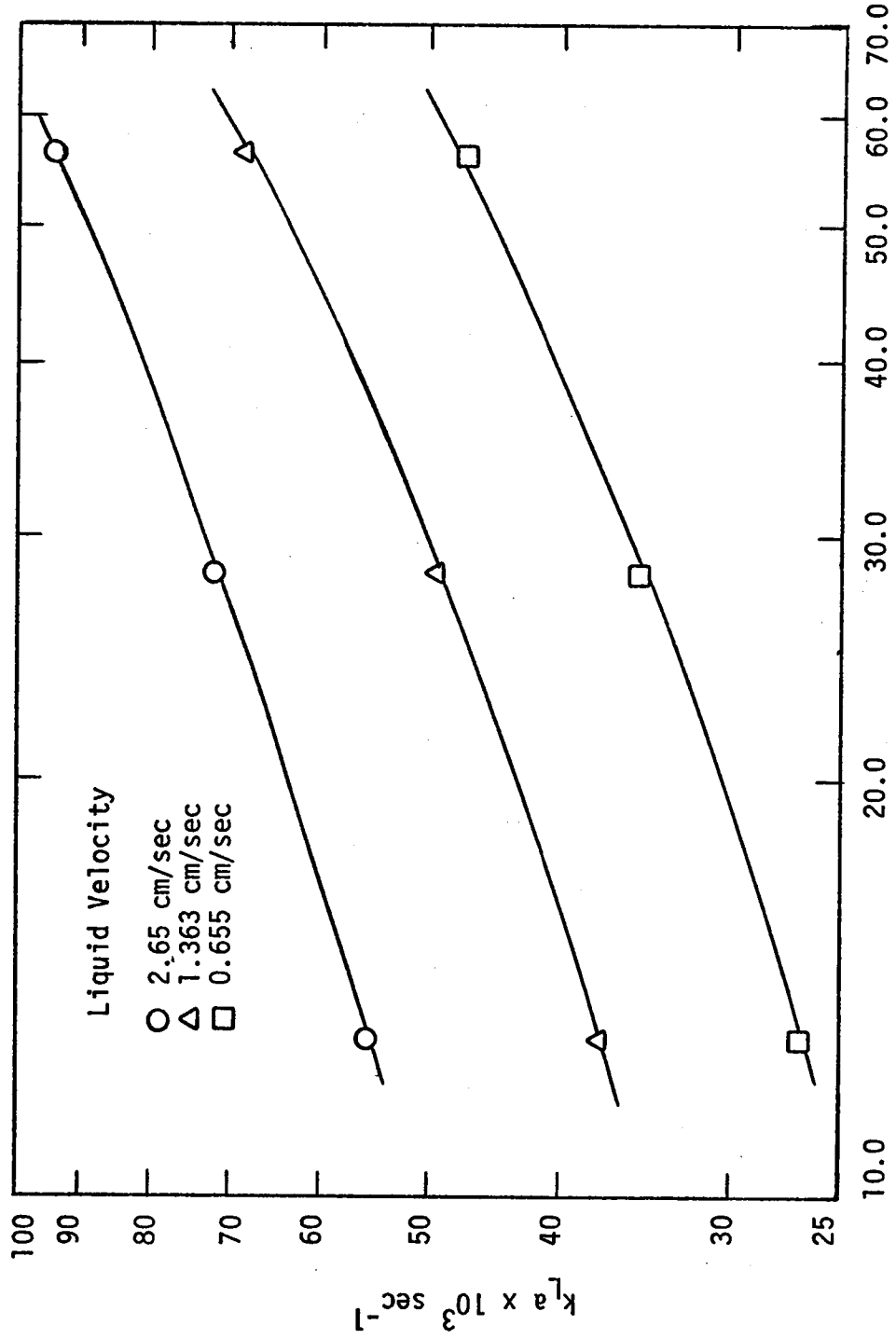


Figure 13. Effect of Gas Superficial Velocity on Liquid-Phase Mass Transfer Coefficient, k_La

C. PULSING FLOW

A pulsing flow effect was observed for the two different heights of packing. This was done by setting a certain liquid rate and then increasing the gas rate and watching the liquid which was collected in the funnel. When pulsing flow was observed, the gas rate was not increased any more, the gas rate and the liquid rate were recorded. This was done for about five different liquid rates.

Graphs of gas flow rates versus liquid flow rates for different height of packing are shown in Figure 14, showing the location of regime of pulsing flow and continuous flow. Pulsing flow was observed by Beimesch and Kessler (3) in concurrent gas-liquid flow in packed beads. They used glass beads and aluminum beads for the packing.

In the present experimental work only two regimes were observed: the pulsing regime and the continuous regime. Spray flow was not observed. It is probably for this reason that the interfacial area of present work does not exceed the geometrical area.

D. EFFECT OF COLUMN HEIGHT

It has often been suggested that the efficiency of a packing decreases as the height of the packed column is increased, the reason being that the liquid finds its way to the wall and runs down it; the flow rate over the packing proper would then decrease, with an adverse effect on both k_L and a. When data were taken in a taller (91.44 cm) column decreases in both k_L and a were observed. Comparison of the

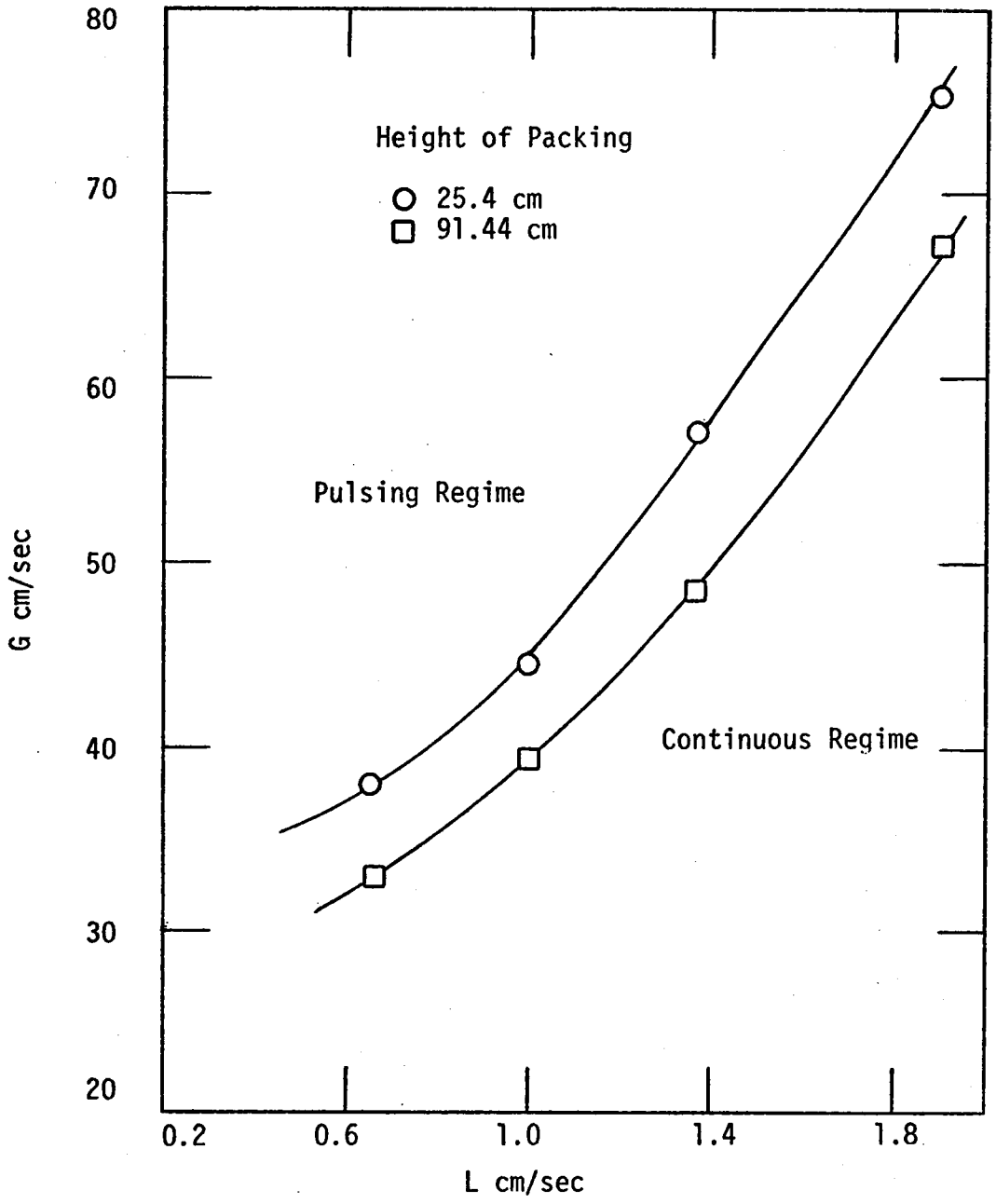


Figure 14. Effect of Gas Velocity and Liquid Velocity on the Flow in the Packed Column

data for the short column and long column are shown in Fiugres 15 and 16. k_L and a were somewhat less in the tall column than in the short column. A number of investigators have shown that, no matter how uniform the distribution of the liquid at the top of the packing, at lower levels there is marked maldistribution (7).

Porter, Barnett and Tepleman (19) examined the channelling of water in packed columns and reported careful observations but were unable to develop a general correlation for the phenomenon. They suggest that the effect of wall flow is significant when the height was over a few tower diameters. They also suggested that wall flow effects decrease as liquid flow increases. Danckwerts and Gillham (8), on the other hand, suggested that the effect is not significant when the height is less than seven column diameters. Wen, et.al. (31) in their investigation of $k_G a$ in concurrent flow found a significant decrease after one foot in a six inch I.D. column packed with one-fourth inch carbon rings and found the effect continued with height.

The observation of the column height effect in the present work agreed with the conclusions of Porter, Barnett and Tepleman (19). The tall column was 9.0 column diameters in length, and a significant effect was produced in the liquid-film mass transfer coefficient and the interfacial area.

E. COMPARISON WITH CHEMICAL ABSORPTION AND PHYSICAL ABSORPTION

Liquid-phase mass transfer coefficients, $k_L a$, for chemical

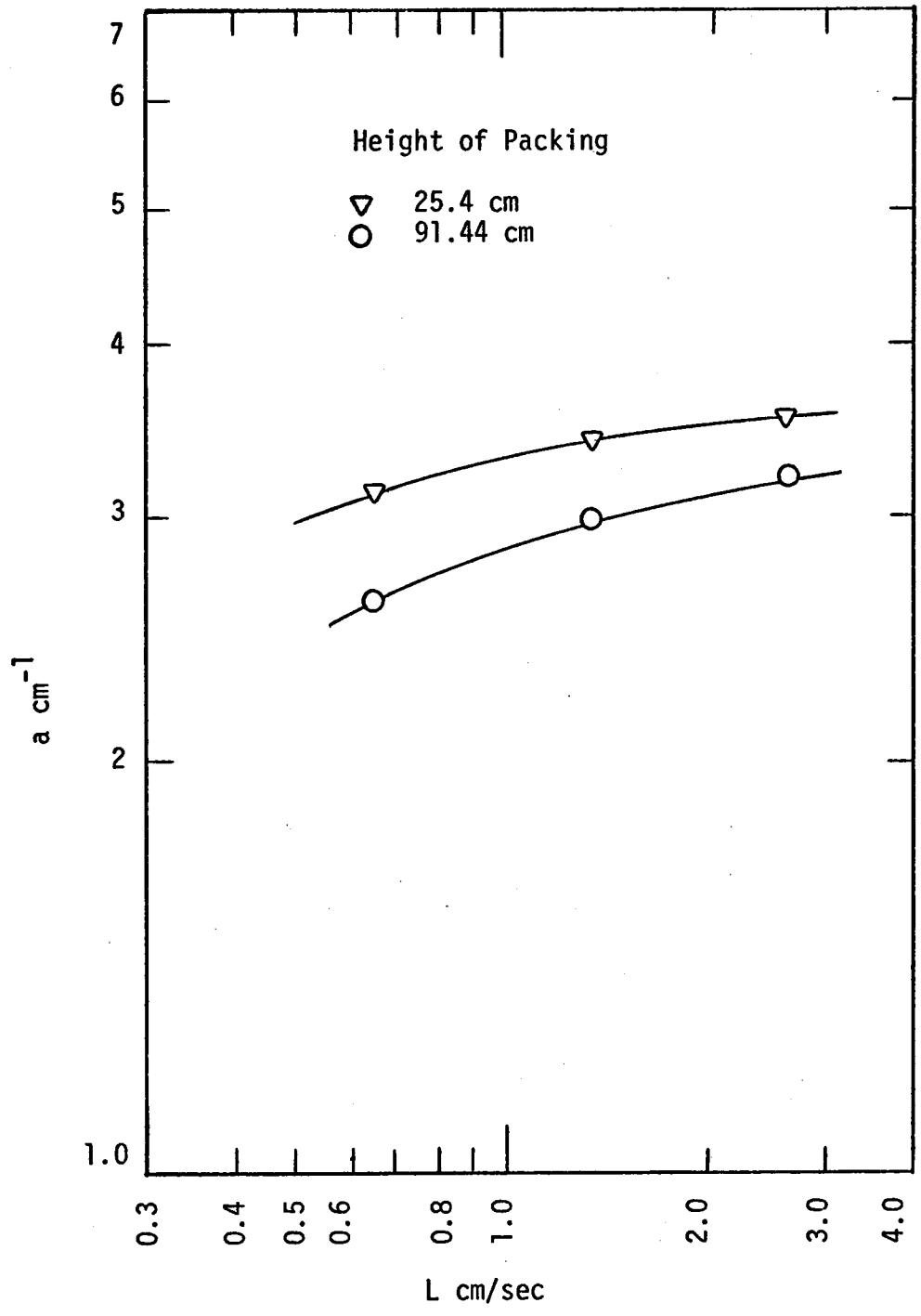


Figure 15. Effect of Height on Effective Interfacial Area

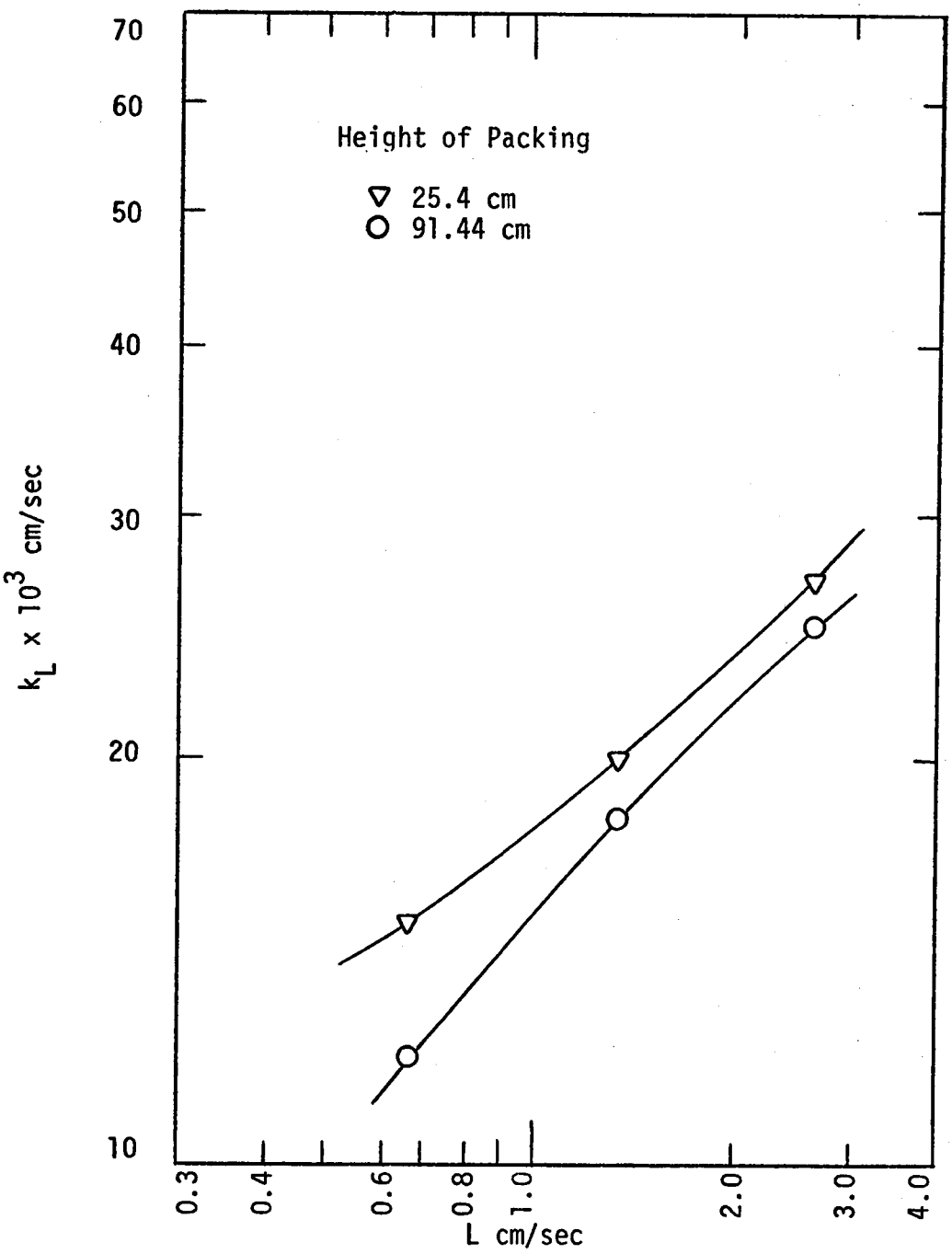


Figure 16. Effect of Height on Liquid-Film Mass Transfer Coefficient, k_L

absorption in the present work and for physical absorption in Ufford's work (30) are shown in Figure 17. Liquid-phase mass transfer coefficients for chemical absorption are higher by a factor of 2.3 at the liquid rate 0.655 cm/sec to 1.3 at the liquid rate 2.65 cm/sec than for physical absorption. This was observed by Joosten and Danckwerts (13) in countercurrent flow. The present work agreed with Joosten and Danckwerts. The difference between both mass transfer coefficients decreases as the liquid rate increases. This was also observed in the present work.

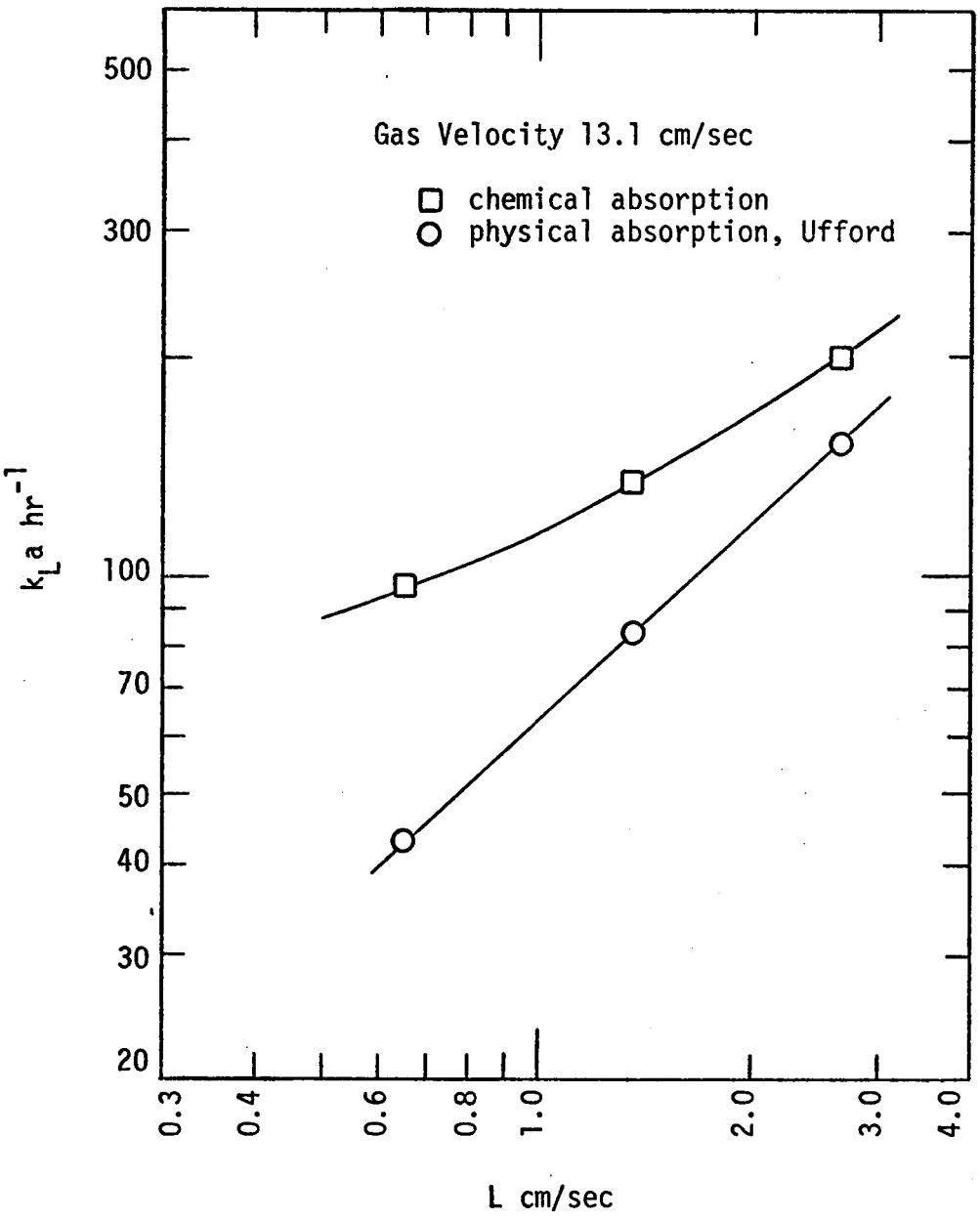


Figure 17. Effect of Chemical Absorption on Liquid-Phase Mass Transfer Coefficient, $k_L a$

CHAPTER V

CONCLUSIONS

The following conclusions were drawn from the results of the present investigation:

(1) Liquid-film mass transfer coefficients, k_L, varied with liquid and gas velocity.

(2) Effective interfacial area, a, varied with liquid and gas velocity.

(3) The effect of liquid velocity on the liquid-film mass transfer coefficient, k_L, is stronger than the gas velocity.

(4) The effect of liquid rate and gas rate on the effective interfacial area, a, is about the same.

(5) In a taller packed tower, k_L, and a, are both less than in a short packed tower.

(6) Liquid-film mass transfer coefficients, $k_L a$, for chemical absorption are higher than for physical absorption. The ratio of $(k_L a)_{chemical}$ to $(k_L a)_{physical}$ decreases as the liquid rate increases.

(7) Pulsing flow was observed at higher gas and lower liquid rate.

(8) The values of k_L and a measured for concurrent flow are not the same as countercurrent flow. Liquid-film mass transfer coefficient, k_L, and interfacial area are higher by roughly a factor of 2.0.

LIST OF REFERENCES

LIST OF REFERENCES

1. Andrieu, J. and Claudel, B., "Measurement of Interfacial Area in a Packed Column by the Sulfite Oxidation Method. Comparison with the Wetted Area," Chem. Engng. Sci., 29, 1263 (1973).

2. Astarita, Giovanni Mass Transfer with Chemical Reaction, New York, Elsevier Publishing Company, (1967).

3. Beimesch, W. E. and Kessler, D. P., "Liquid-Gas Distribution Measurements in the Pulsing Regime of Two-Phase Concurrent Flow in Packed Beds," AIChE Journal, 17, 1160, (1971).

4. Comstock, C. S. and Dodge, B. F., "Rate of Carbon Dioxide Absorption by Carbonate Solutions in a Packed Tower," Ind. Engr. Chem., 29, 520, (1937).

5. Danckwerts, P. V., Kennedy, A. M., and Roberts, D., "Kinetics of CO_2 Absorption in Alkaline Solutions-II," Chem. Engng, Sci., 18, 63, (1963).

6. Danckwerts, P. V. and Rizvi, S. F., "The Design of Gas Absorbers, Part II: Effective Interfacial Area for Several Types of Packing," Trans. Instn. Chem. Engrs., 49, 124, (1971).

7. Danckwerts, P. V. Gas-Liquid Reactions, New York, McGraw-Hill Book Company, (1970).

8. Danckwerts, P. V. and Gillham, A. J., "The Design of Gas Absorbers, I-Methods for Predicting Rates of Absorption with Chemical Reaction in Packed Columns, and Tests with One-Half Inch Raschig Rings," Trans. Instn. Chem. Engrs. (British), 44, T42, (1966).

9. Danckwerts, P. V. and Sharma, M. M., "The Absorption of Carbon Dioxide into Solutions of Alkalis and Amines," Chem. Engr., CE244, (1966).

10. Dodds, W. S., Stutzman, L. F., Sollami, B. J., and McCarter, R. J., "Cocurrent Gas Absorption Mass Transfer," AIChE Journal, 6, 197, (1960).

11. Fisher, R. B. and Peters, D. G. Quantitative Chemical Analysis, Philadelphia, W. B. Saunders Company, (1968).

12. Gianetto, A., Specchia, V., and Baldi, G., "Absorption in Packed Towers with Concurrent Downward High-Velocity Flows-II: Mass Transfer," AIChE Journal, 10, 916, (1973).

13. Joosten, G. E. H. and Danckwerts, P. V., "Chemical Reaction and Effective Interfacial Areas in Gas Absorption," Chem. Engng. Sci., 28, 453, (1973).

14. Larkins, R. P., White, R. R., and Jeffrey, D. W., "Two-Phase Concurrent Flow in Packed Beds," AIChE Journal, 7, 231, (1961).

15. Onda, K., Takenchi, H., Maeda, Y., and Takeuchi, N., "Liquid Distribution in a Packed Column," Chem. Engng. Sci., 28, 1677, (1973).

16. Onda, K., Sada, E., and Murase, Y., "Liquid-Side Mass Transfer Coefficients in Packed Towers," AIChE Journal, 5, 235, (1959).

17. Payne, J. W. and Dodge, B. F., "Rate of Absorption of Carbon Dioxide in Water and in Alkaline Media," Ind. Engr. Chem., 24, 630, (1932).

18. Perry, R. H., Chilton, C. M., and Kirkpatrick, S. D. Chemical Engineers' Handbook, New York, McGraw-Hill Book Company (1963).

19. Porter, K. E. and Tepleman, J. J., "Liquid Flow in Packed Columns, Part III: Wall Flow," Trans, Instn. Chem. Engrs., 46, T86, (1968).

20. Puranik, S. S. and Vogelpohl, A., "Effective Interfacial Area in Irrigated Packed Columns," Chem. Engng. Sci., 29, 501, (1974).

21. Ratcliff, G. A. and Holdcroft, J. G., "Diffusivities of Gases in Aqueous Electrolyte Solutions," Trans. Instn. Chem. Engrs., 41, 315, (1963).

22. Reiss, L. P., "Cocurrent Gas-Liquid Contacting in Packed Columns," I and E. C. Process Design and Development, 6, 486, (1967).

23. Richards, G. M., Ractliff, G. A. and Danckwerts, P. V., "Kinetics of CO_2 Absorption-III, First-Order Reaction in a Packed Column," Chem. Engr. Sci., 19, 325, (1964).

24. Roberts, D. and Danckwerts, P. V., "Kinetics of CO_2 Absorption in Alkaline Solutions-I," Chem. Engr. Sci., 17, 961, (1962).

25. Scott, W. W. and Furman, N. H., eds. Standard Methods of Chemical Analysis, New York, Van Nostrand Company, (1939).

26. Sherwood, T. K. and Holloway, F. A. L., "Performance of Packed Towers--Liquid Film Data for Several Packings," Trans. AIChE, 36, 39, (1939).

27. Shulman, H. L., Ullrich, C. F., Proulx, A. Z., and Zimmerman, J. O., "Wetted and Effective Interfacial Areas, Gas- and Liquid-Phase Mass Transfer Rates," AIChE Journal, 1, 253, (1955).

28. Tavares Da Silva, A. and Danckwerts, P. V., "The Effect of Halogens on the Rate of Absorption of Carbon Dioxide," Chem. Engr. Sci., 28, 847, (1973).

29. Treybal, R. E. Mass Transfer Operations, New York, McGraw-Hill Book Company, (1968).

30. Ufford, R., "Liquid Phase Mass Transfer Coefficients in Cocurrent Flow Gas Absorption in a Packed Column at High Liquid Flow Rates," M.S. Thesis, The University of Tennessee, (1973).

31. Wen, C. Y., O'Brien, W. S., and Fan, Liang-Tseng, "Mass Transfer in Packed Beds Operated Cocurrently," J. Chem. Engr. Data, 8, 42, (1963).

32. Yoshida, F. and Miura, T., "Effective Interfacial Area in Packed Columns for Absorption with Chemical Reaction," AIChE Journal, 9, 331, (1963).

APPENDICES

APPENDIX A

APPENDIX A

SAMPLE CALCULATIONS

The following is the calculation to show, liquid-side is controlling, reaction is a pseudo first order and calculation of liquid-film mass transfer coefficient and interfacial area.

SAMPLE CALCULATIONS

A. CALCULATION TO SHOW LIQUID-SIDE IS CONTROLLING

Calculate Solubility of CO_2 in 0.207M Na_2CO_3 and 0.215M $NaHCO_3$

Van Kraevelen and Hoftijzer.

$$\log_{10} (He/He^\circ) = hI \tag{1}$$

$$I = \frac{1}{2} \Sigma C_i z_i^2 \tag{2}$$

I = ionic strength.

He° = Henry's law constant in water.

The quantity h is the sum of contributions referring to the species of positive and of negative ions present and to the species of gas.

$$h = h_+ + h_- + h_G \tag{3}$$

$$\log_{10} (He/He^\circ) = h_1 I_1 + h_2 I_2 = 0.093[0.621 + 0.215]$$

$$\log_{10} (He/He^\circ) = 0.07775$$

$$\frac{He}{He^\circ} = 1.96$$

$$\frac{1}{He^{\circ}} = 0.034 \ \frac{\text{gm moles}}{\text{liter atm}} \qquad \text{From Perry's}$$

$$He = \frac{1.96}{0.034}$$

$$\frac{1}{He} = 0.0289 \ \text{gm moles/liter atm}$$

$$A^* = \frac{p_i}{He}$$

$$P_i = x_A P$$

P = total pressure

x_A = mole fraction of CO_2 in gas mixture which is ten percent

$x_A = 0.1$

P = 0.98 atm

A* = 0.00284 gm moles/ liter

$A^* = 2.84 \times 10^{-6}$ gm moles/cm^3

Diffusivity Calculation

Ratcliff and Holdcroft [21].

$$\log_{10} (D_o/D) = 0.637 \log_{10} (\frac{\mu}{\mu_o}) \qquad (4)$$

μ = viscosity of solution (g/cm sec or cp)

μ_o = viscosity of water (g/cm sec or cp)

D = diffusivity (cm^2/sec)

D_o = diffusivity in water (cm^2/sec)

D_o = 1.92×10^{-5} cm^2/sec and viscosities from Perry's

$$\log\left(\frac{1.92 \times 10^{-5}}{D}\right) = 0.637 \log_{10}\left(\frac{1.17}{0.8937}\right)$$

$$D = 1.62 \times 10^{-5} \text{ cm}^2/\text{sec}$$

$$A^* \sqrt{D} = 11.43 \times 10^{-9} \frac{\text{gm moles}}{\text{cm}^2 \text{ sec}^{1/2}}$$

Diffusivity of Gases

Hirschfelder, Bird and Spotz Perry's 14-20.

$$D_G = \frac{BT^{3/2}\left(\frac{1}{M_1} + \frac{1}{M_2}\right)}{Pr_{12}^2 I_D} \qquad (5)$$

$$B = (10.7 - 2.46 \quad \frac{1}{M_1} + \frac{1}{M_2}) \times 10^{-4}$$

r_{12}= collision diameter, angstroms

I_D = collision integral for diffusion, function of KT/e_{12}

k = Boltzmann constant

e_{12}= energy of molecular interaction, ergs

$$D_G = \frac{10.11 \times 10^{-4} [298]^{3/2} \quad \frac{1}{28.97} + \frac{1}{44}}{0.98 \times [3.8]^2 \times 2.195}$$

$= 0.04 \text{ cm}^2/\text{sec}$

Viscosity of Gas

From Perry's 3-230.

$$\mu^{\circ}_{m} = \frac{\Sigma y_i \mu_i (M_i)^{1/2}}{\Sigma y_i (M_i)^{1/2}} \qquad (6)$$

Viscosity Values from Perry's 3-197.

$$\mu^{\circ}_{m} = \frac{0.9 \times 0.0168 \times (28.97)^{1/2} + 0.1\ (0.0145)\ (44)^{1/2}}{0.9 \times (28.97)^{1/2} + (0.1)\ (44)^{1/2}}$$

$$= 0.0165 \text{ ceptipoise}$$

$$\rho_G = 1.22 \times 10^{-3} \text{ gm/cm}^3$$

From Treybal [29] for Countercurrent.

$$\frac{k_G p_{BM} S_{c_G}^{2/3}}{G} = 1.195 \left[\frac{ds\ G'}{\mu_G''(1-e)}\right]^{-0.36} \qquad (7)$$

where

G = superficial molar gas velocity, g moles/sec cm^2

G' = superficial gas mass velocity, gm/sec cm^2

d_s = diameter of a sphere of same surface as a single packing particle, ft

Sc = Schmidt number, $\mu''/\rho D$, dimensionless

μ''_G = viscosity, gm/cm sec

p_{BM} = logarithmic mean partial pressure of non-diffusing gas, atm

For runs of gas rate 13.1 cm/sec and liquid rate 0.655 cm/sec

$$\frac{k_G p_{BM} \left[\frac{0.000165}{1.22 \times 10^{-3} \times 0.04}\right]^{2/3}}{52.4 \times 10^{-5}} = 1.195 \left[\frac{0.0582 \times 30.48 \times 0.016}{0.000165(1 - 0.63)}\right]^{-0.36}$$

$$k_G p_{BM} = 2.544 \times 10^{-5} \ \frac{\text{gm moles}}{\text{sec cm}^2}$$

Total pressure = 0.98 atm.

$$p_{BM} = \frac{0.90776 \times 0.98 - 0.9 \times 0.98}{\ln \left(\frac{0.90776 \times 0.98}{0.9 \times 0.98}\right)}$$

$$= 0.886 \text{ atm.}$$

$$k_G = 2.87 \times 10^{-5} \ \frac{\text{gm moles}}{\text{sec cm}^2}$$

<u>k_L for Countercurrent Flow.</u>

From Figure 9, Richards, et.al. [23]

$$k_L = 7.67 \times 10^{-3} \text{ cm/sec}$$

$$\frac{1}{He} = 2.89 \times 10^{-5} \ \frac{\text{gm moles}}{\text{cm}^2 \text{ sec atm}}$$

To say liquid side is controlling,

$$k_G \gg \frac{k_L}{He} \quad \text{must be true.} \tag{8}$$

$$\frac{k_L}{He} = 7.67 \times 10^{-3} \times 2.89 \times 10^{-5}$$

$$= 22.2 \times 10^{-8} \frac{\text{gm moles}}{\text{cm}^2 \text{ sec atm}}$$

$$2.87 \times 10^{-5} \gg 2.22 \times 10^{-7}$$

This is done in countercurrent operation because there was not any correlation available in concurrent operation for k_G.

Value of $\frac{k_L}{He}$ in the Present Work.

$$\frac{k_L}{He} = 13.16 \times 10^{-3} \times 2.89 \times 10^{-5}$$

$$= 3.8 \times 10^{-7} \frac{\text{gm moles}}{\text{cm}^2 \text{ sec atm}}$$

$$2.87 \times 10^{-5} \gg 3.8 \times 10^{-7}$$

B. CALCULATION TO SHOW REACTION IS A PSEUDO-FIRST ORDER

For Reaction to Be Pseudo First Order

$$\sqrt{1 + \frac{D_A k_1}{k_L^2}} - 1 \ll \frac{B^\circ}{A^*} \tag{9}$$

$D_A = 1.62 \times 10^{-5}$ cm^2/sec

$k_1 = 38$ sec^{-1} taken as an average rate of different catalyst concentration

$k_L = 26.85 \times 10^{-3}$ cm/sec for gas rate 56.47 cm/sec and liquid rate 2.65 cm/sec

$$\sqrt{1 + \frac{1.62 \times 10^{-5} \times 38}{72.2 \times 10^{-5}}} - 1 \ll \frac{0.207}{0.00284}$$

$0.36 \ll 72.89$

C. CALCULATION OF LIQUID-FILM MASS TRANSFER COEFFICIENTS AND INTERFACIAL AREA

Calculation for Run 1

Liquid Flow Rate 5000 lb/hr ft^2 from Figure 18.

$l = 5000$ lb/hr ft^2 $= 2441.25$ gm/hr cm^2

$= 0.678$ gm/cm^2 sec

$\rho_{avg} = 1.035$ gm/cm^3

$L = 0.655$ cm/sec

Air Flow Rate 3.48 lb moles/hr ft^2 from Figure 20.

CO_2 17 lb/hr ft^2 from Figure 19

Height of the packing = 25.4 cm

$$\text{Air flow rate} = 3.48 \frac{\text{lb moles}}{\text{hr ft}^2} = 1.86 \times 10^{-5} \frac{\text{gm moles}}{\text{cu cm sec}}$$

CO_2 flow rate 17 lb/hr ft^2 = 2.06×10^{-6} GM moles/cu cm sec

$$\text{Total gas flow rate} = 2.066 \times 10^{-5} \frac{\text{GM moles}}{\text{cu cm sec}}$$

$\rho_G = 0.00122 \text{ gm/cm}^3$

G = 13.1 cm/sec

Calculate Molarity of Na_2CO_3.

Molarity of HCl = 0.03017 gm moles/liter 5 ml of sample

For Run 2 0.01M Catalyst Concentration

Amount of HCl Required for First Equivalent Point from the Curve 34.33 ml.

$$\text{Molarity of } Na_2CO_3 = 0.20716 \frac{\text{gm moles}}{\text{liter}} \quad \text{Input}$$

$$\text{Molarity of } Na_2CO_2 = 0.20194 \frac{\text{gm moles}}{\text{liter}} \quad \text{Output}$$

Amount of CO_2 Absorbed.

$$Ra = \frac{[0.20716 - 0.20194] \times 0.655 \times 10^{-3}}{25.4 \text{ cm length}}$$

$$= 1.34 \times 10^{-7} \text{ gm moles/sec cm}^3$$

$$k_1 = k_L [OCl]$$

$$CO_3^{--} = \frac{0.20716 + 0.20194}{2} \frac{\text{gm moles}}{\text{liter}}$$

$$k_1 = 2100[0.01]$$

$$k_1 = 21.0 \text{ sec}^{-1}$$

From Figure 4 For Liquid Rate 0.655 cm/sec.

$$\text{Intercept} = 0.5766 \times 10^{-14} \left[\frac{\text{gm moles}}{\text{cm}^3 \text{ sec}}\right]^2$$

$$\text{Slope} = 6.820 \times 10^{-6} \left[\frac{\text{gm moles}}{\text{cm}^3}\right]^2 \frac{1}{\text{sec}}$$

$$\text{Slope} = [a A^*]^2 D$$

$$\sqrt{\text{slope}} = a A^* \sqrt{D}$$

$$a = \frac{[6.818 \times 10^{-16}]^{1/2}}{11.43 \times 10^{-9}}$$

$$= 2.28 \text{ cm}^2/\text{cm}^3$$

$$\sqrt{\text{intercept}} = k_L \, a \, A^*$$

$$k_L = \frac{[0.5766 \times 10^{-14}]^{1/2}}{2.28 \times 2.84 \times 10^{-6}} = 11.72 \times 10^{-3} \text{ cm/sec}$$

APPENDIX B

APPENDIX B

SUPPLEMENTARY FIGURES

The following figures are the rotameter calibration curves developed during the course of the experimental work of this project.

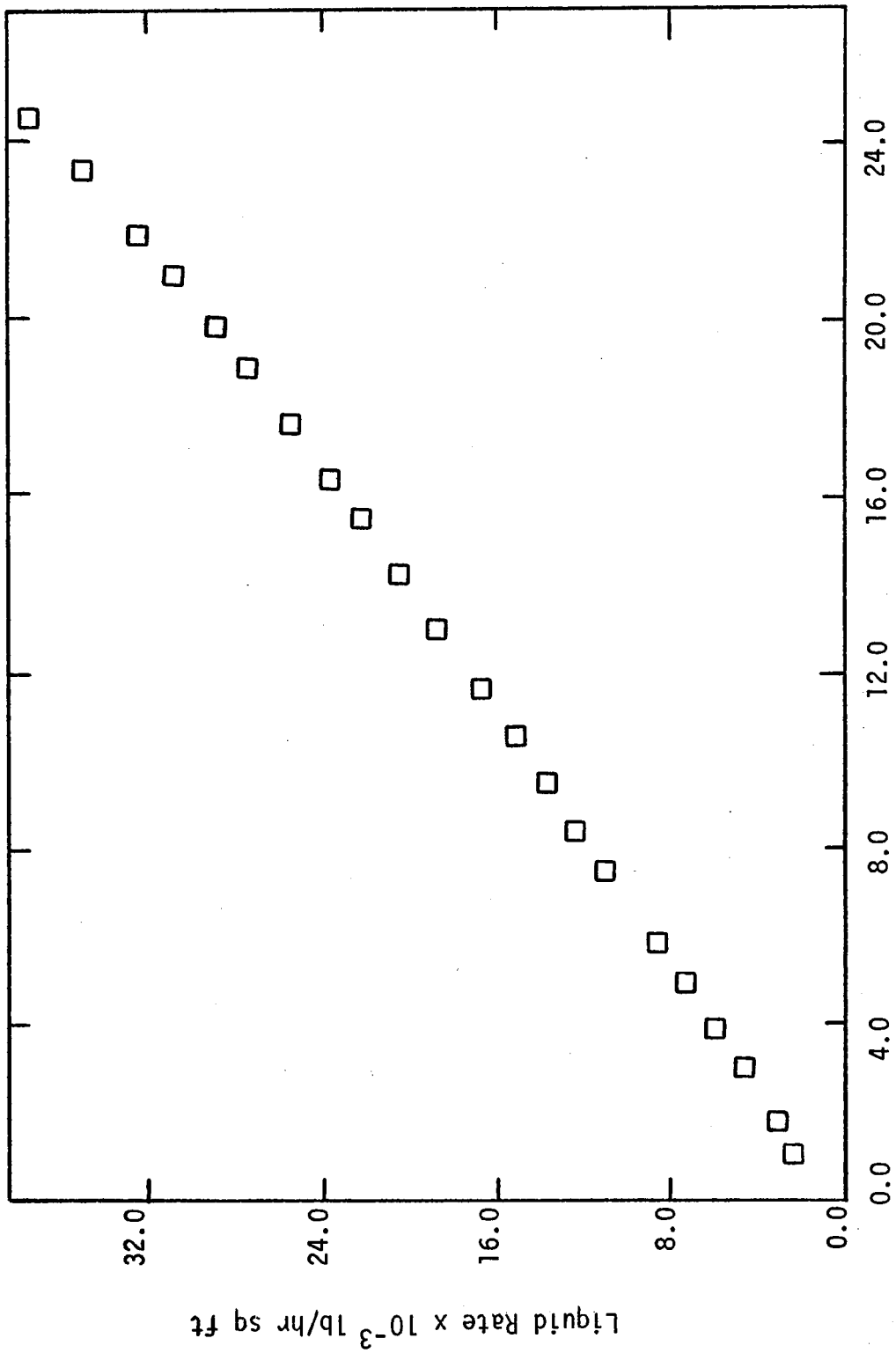


Figure 18. Liquid Rotameter Calibration Curve

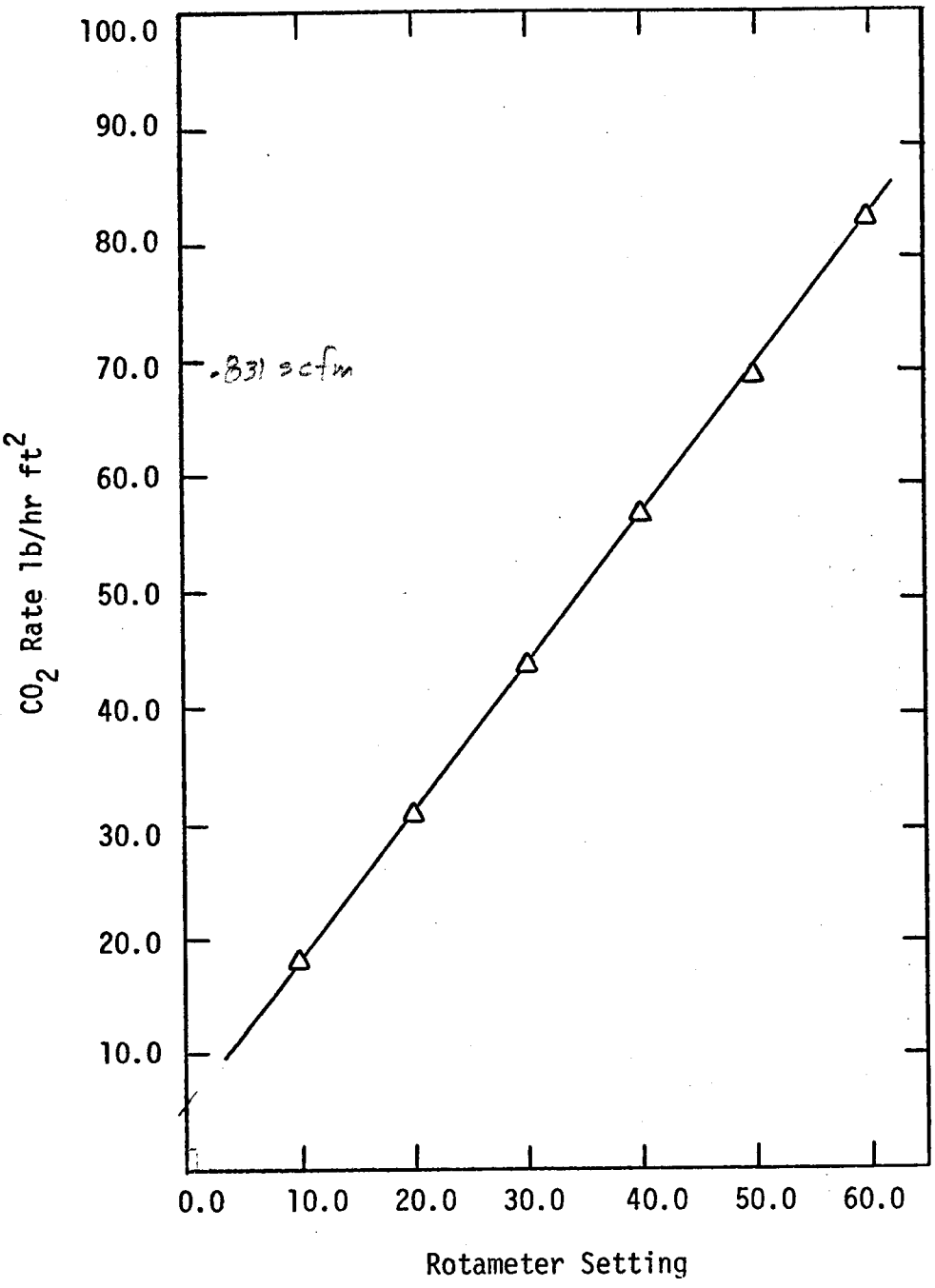


Figure 19. CO_2 Rotameter Calibration Curve

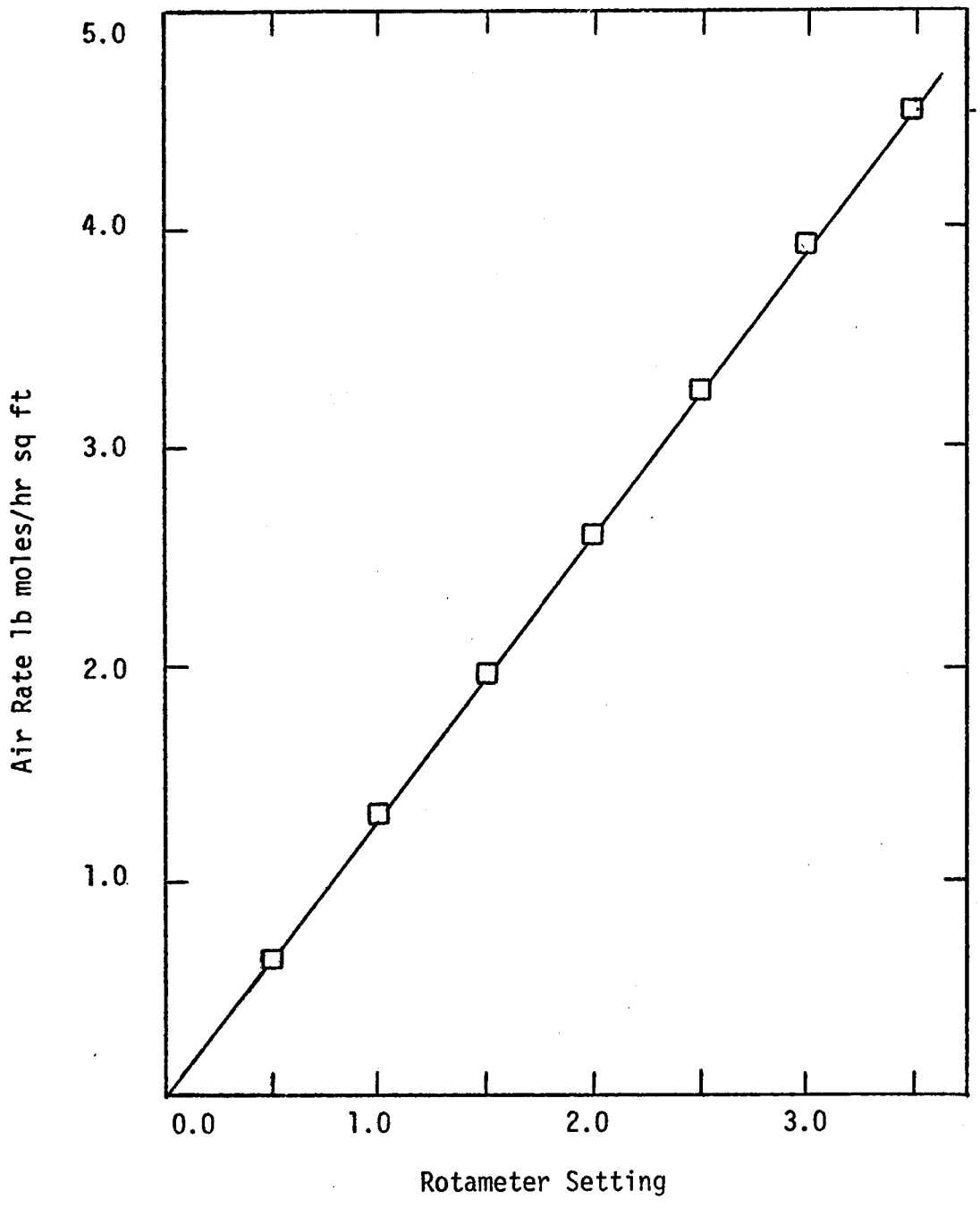


Figure 20. First Air Rotameter Calibration Curve

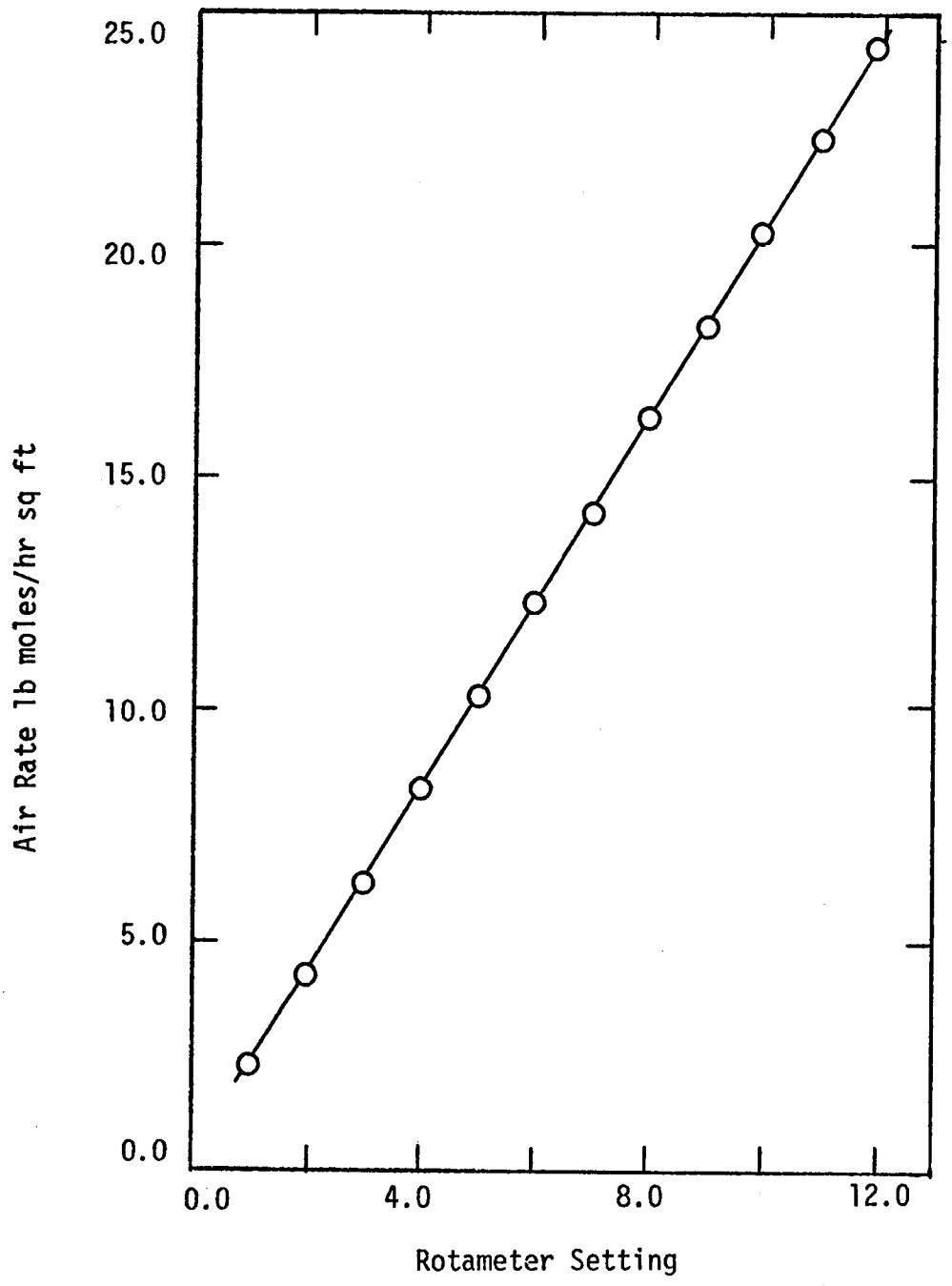


Figure 21. Second Air Rotameter Calibration Curve

APPENDIX C

APPENDIX C

ORIGINAL DATA

Tables 1 through 4 present the liquid superficial velocity, gas superficial velocity, carbon dioxide flow rate, air flow rate, concentration of Na_2CO_3 in input and output streams and rate of absorption determined in the analysis for each of the runs of this project.

TABLE 1

GAS SUPERFICIAL VELOCITY 13.1 CM/SEC

WITH HEIGHT OF PACKING = 25.4 CM

Run	Liquid Superficial Velocity cm/sec	Concentration of Na_2CO_3 Input $\frac{gm\ moles}{liter}$	Concentration of Na_2CO_3 Output $\frac{gm\ moles}{liter}$	First-Order Constant k_1 sec^{-1}	Rate of Absorption $\frac{gm\ moles}{cu\ cm\ sec}$
1	0.655	0.2810	0.20507	0	0.774×10^{-7}
2	0.655	0.20716	0.26194	21.0	1.34×10^{-7}
3	0.655	0.20950	0.202	42.5	1.94×10^{-7}
4	0.655	0.20617	0.19766	61.1	2.19×10^{-7}
5	0.655	0.20855	0.19962	70.75	2.3×10^{-7}
6	1.363	0.20552	0.20366	0	0.998×10^{-7}
7	1.363	0.20727	0.20388	21.2	3.3×10^{-7}
8	1.363	0.20815	0.20388	42.4	5.26×10^{-7}
9	1.363	0.20923	0.20448	61.0	6.5×10^{-7}
10	1.363	0.20835	0.20311	71.0	7.9×10^{-7}
11	2.65	0.2073	0.20577	0	1.6×10^{-7}
12	2.65	0.20814	0.20606	21.0	2.17×10^{-7}
13	2.65	0.209	0.20642	42.5	2.68×10^{-7}
14	2.65	0.20565	0.20272	61.0	3.05×10^{-7}
15	2.65	0.20825	0.20515	71.5	3.2×10^{-7}

Note: Air flow rate = 1.86×10^{-5} $\frac{gm\ moles}{cu\ cm\ sec}$; carbon dioxide flow rate = 2.06×10^{-6} $\frac{gm\ moles}{cu\ cm\ sec}$.

TABLE 2

GAS SUPERFICIAL VELOCITY 28.25 CM/SEC

WITH HEIGHT OF PACKING = 25.4 CM

Run	Liquid Superficial Velocity cm/sec	Concentration of Na_2CO_3 Input $\frac{gm\ moles}{liter}$	Concentration of Na_2CO_3 Output $\frac{gm\ moles}{liter}$	First-Order Constant k_1 sec^{-1}	Rate of Absorption $\frac{gm\ moles}{cu\ cm\ sec}$
16	0.655	0.20737	0.20359	0	0.975×10^{-7}
17	0.655	0.20645	0.19974	20.9	1.73×10^{-7}
18	0.655	0.20815	0.19964	41.5	2.195×10^{-7}
19	0.655	0.20780	0.19788	61.5	2.56×10^{-7}
20	1.363	0.20817	0.20548	0	1.442×10^{-7}
21	1.363	0.20734	0.20338	21.0	2.13×10^{-7}
22	1.363	0.20638	0.20130	42.5	2.72×10^{-7}
23	1.363	0.20810	0.2023	62.0	3.11×10^{-7}
24	2.65	0.20823	0.20626	0	2.05×10^{-7}
25	2.65	0.2074	0.2049	21.2	2.63×10^{-7}
26	2.65	0.20635	0.20338	42.5	3.10×10^{-7}
27	2.65	0.205	0.20166	61.5	3.48×10^{-7}

Note: Air flow rate = 4.0×10^{-5} $\frac{gm\ moles}{cu\ cm\ sec}$; carbon dioxide flow rate = 4.46×10^{-6} $\frac{gm\ moles}{cu\ cm\ sec}$.

TABLE 3

GAS SUPERFICIAL VELOCITY 56.5 CM/SEC

WITH HEIGHT OF PACKING = 25.4 CM

Run	Liquid Superficial Velocity cm/sec	Concentration of Na_2CO_3 Input $\frac{gm\ moles}{liter}$	Concentration of Na_2CO_3 Outputs $\frac{gm\ moles}{liter}$	First-Order Constant k_1 sec^{-1}	Rate of Absorption $\frac{gm\ moles}{cu\ cm\ sec}$
28	0.655	0.20834	0.203	0	1.38×10^{-7}
29	0.655	0.20737	0.19933	20.7	2.074×10^{-7}
30	0.655	0.207	0.1967	41.2	2.646×10^{-7}
31	0.655	0.2065	0.1945	62.0	3.11×10^{-7}
32	1.363	0.20634	0.20274	0	1.9365×10^{-7}
33	1.363	0.20535	0.20045	20.5	2.63×10^{-7}
34	1.363	0.207	0.201	42.0	3.21×10^{-7}
35	1.363	0.20635	0.19957	62.2	3.64×10^{-7}
36	2.65	0.20837	0.20680	0	2.68×10^{-7}
37	2.65	0.20758	0.20444	21.0	3.27×10^{-7}
38	2.65	0.20780	0.20420	41.0	3.75×10^{-7}
39	2.65	0.20600	0.202	62.5	4.19×10^{-7}

Note: Air flow rate = 8.0×10^{-5} $\frac{gm\ moles}{cu\ cm\ sec}$; carbon dioxide flow rate = 8.89×10^{-6} $\frac{gm\ moles}{cu\ cm\ sec}$.

TABLE 4

GAS SUPERFICIAL VELOCITY 56.5 CM/SEC

WITH HEIGHT OF PACKING = 91.44 CM

Run	Liquid Superficial Velocity cm/sec	Concentration of Na_2CO_3 Input $\frac{gm\ moles}{liter}$	Concentration of Na_2CO_3 Outputs $\frac{gm\ moles}{liter}$	First-Order Constant k_1 sec^{-1}	Rate of Absorption $\frac{gm\ moles}{cu\ cm\ sec}$
40	0.655	0.2074	0.1944	0	0.934×10^{-7}
41	0.655	0.20637	0.18427	20.4	1.58×10^{-7}
42	0.655	0.2068	0.1785	40.4	2.03×10^{-7}
43	0.655	0.207	0.1724	60.30	2.5×10^{-7}
44	1.363	0.2087	0.1983	0	1.55×10^{-7}
45	1.363	0.2075	0.1927	20.5	2.21×10^{-7}
46	1.363	0.2068	0.1886	40.7	2.71×10^{-7}
47	1.363	0.20734	0.1866	61.0	3.10×10^{-7}
48	2.65	0.20537	0.19723	0	2.356×10^{-7}
49	2.65	0.20648	0.19660	20.7	2.86×10^{-7}
50	2.65	0.20726	0.19580	41.0	3.32×10^{-7}
51	2.65	0.2088	0.1962	61.2	3.654×10^{-7}

Note: Air flow rate = 2.22×10^{-5} $\frac{gm\ moles}{cu\ cm\ sec}$; carbon dioxide flow rate = 2.47×10^{-6} $\frac{gm\ moles}{cu\ cm\ sec}$.

APPENDIX D

APPENDIX D

CALCULATED RESULTS

Tables 5 and 6 present liquid superficial velocity, gas superficial velocity, and calculated intercept and slope of the line. Tables 7 and 8 present liquid superficial velocity, gas superficial velocity and calculated liquid-film mass transfer coefficient, k_L, and effective interfacial area, a.

TABLE 5

CALCULATED INTERCEPT AND SLOPE OF THE LINE

FOR HEIGHT OF PACKING = 25.4 CM

Liquid Superficial Velocity cm/sec	Gas Superficial Velocity cm/sec	Intercept of the line $[\frac{\text{gm moles}}{\text{cu cm sec}}]^2 \times 10^{14}$	Slope of the Line $[\frac{\text{gm moles}}{\text{cu cm}}]^2 \frac{1}{\text{sec}} \times 10^{16}$
0.655	13.1	0.576	6.82
1.363	13.1	1.14	9.33
2.65	13.1	2.5	10.9
0.655	28.25	1.08	9.33
1.363	28.25	2.0	12.3
2.65	28.25	4.2	12.7
0.655	56.5	1.81	12.8
1.363	56.5	3.8	15.28
2.65	56.5	7.3	16.37

TABLE 6

CALCULATED INTERCEPT AND SLOPE OF THE LINE

FOR HEIGHT OF PACKING = 91.44 CM

Liquid Superficial Velocity cm/sec	Gas Superficial Velocity cm/sec	Intercept of the line $[\frac{\text{gm moles}}{\text{cu cm sec}}]^2 \times 10^{14}$	Slope of the Line $[\frac{\text{gm moles}}{\text{cu cm}}]^2 \frac{1}{\text{sec}} \times 10^{16}$
0.655	56.5	0.8	9.0
1.363	56.5	2.4	11.8
2.65	56.5	5.37	13.4

TABLE 7

CALCULATED EFFECTIVE INTERFACIAL AREAS AND LIQUID-FILM MASS TRANSFER COEFFICIENTS FOR HEIGHT OF PACKING = 25.4 CM

Liquid Superficial Velocity cm/sec	Gas Superficial Velocity	Effective Interfacial Area, a, cm^{-1}	Liquid-Film Mass Transfer Coefficient, k_L, cm/sec x 10^3
0.655	13.1	2.28	11.72
1.363	13.10	2.67	14.1
2.65	13.1	2.89	19.25
0.655	28.25	2.67	13.16
1.363	28.25	3.07	16.21
2.65	28.25	3.12	23.10
0.655	56.5	3.13	15.08
1.363	56.5	3.42	20.0
2.65	56.5	3.54	26.85

TABLE 8

CALCULATED EFFECTIVE INTERFACIAL AREAS AND LIQUID-FILM MASS TRANSFER COEFFICIENTS FOR HEIGHT OF PACKING = 91.44 CM

Liquid Superficial Velocity cm/sec	Gas Superficial Velocity	Effective Interfacial Area, a, cm^{-1}	Liquid-Film Mass Transfer Coefficients, k_L, cm/sec x 10^3
0.655	56.5	2.62	12.0
1.363	56.5	3.0	18.17
2.65	56.47	3.2	25.5

VITA

The author was born on August 18, 1949, in Bombay, India. He came to the United States in February 1968.

He graduated from E. T. High School (India) in June 1966. He transferred from the University of Wisconsin to the University of Tennessee in the fall of 1970. While an undergraduate the author became a member of Tau Beta Pi. In March 1972, he received his Bachelor of Science degree, and in the fall of 1972 he entered the Graduate School at the University of Tennessee. He received the Master of Science degree with a major in Chemical Engineering in December 1974.